Hydrosilylation of Terminal Alkynes Catalyzed by a ONO-Pincer Iridium(III) Hydride Compound: Mechanistic Insights into the Hydrosilylation and Dehydrogenative Silylation Catalysis

Jesús J. Pérez-Torrente,[*,†] *Duc Hanh Nguyen,*[‡] *M. Victoria Jiménez,*[†] *F. Javier Modrego,*[*,†] *Raquel Puerta-Oteo,*[†] *Daniel Gómez-Bautista,*[†] *Manuel Iglesias*[†] *and Luis A. Oro*[†]

[†] Departamento de Química Inorgánica, Instituto de Síntesis Química y Catálisis Homogénea–ISQCH, Universidad de Zaragoza–CSIC, Facultad de Ciencias, C/ Pedro Cerbuna, 12, 50009 Zaragoza, Spain.

[‡] Univ. Lille, CNRS, Centrale Lille, ENSCL, Univ. Artois, UMR 8181, Unité de Catalyse et Chimie du Solide (UCCS). F-59000 Lille, France.

Keywords

Hydrosilylation, dehydrogenative silylation, alkynes, iridium, pincer, metallacyclopropene, mechanism, DFT

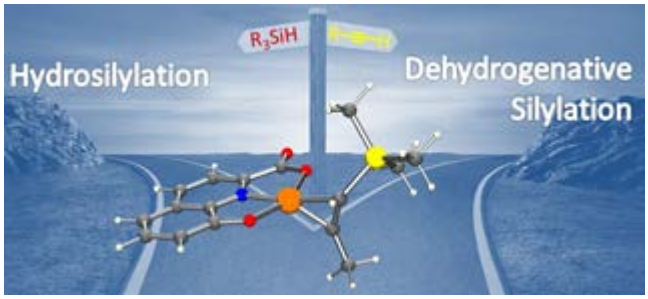

Abstract

The catalytic activity in the hydrosilylation of terminal alkynes by the unsaturated hydrido iridium(III) compound [IrH(κ^3-hqca)(coe)] (**1**), which contains the rigid asymmetrical dianionic ONO pincer ligand 8-oxidoquinoline-2-carboxylate, has been studied. A range of aliphatic and aromatic 1-alkynes has been efficiently reduced using various hydrosilanes. Hydrosilylation of linear 1-alkynes, hex-1-yne or oct-1-yne, gives a good selectivity towards the β-(*Z*)-vinylsilane product while for the bulkier *t*-Bu-C≡CH a reverse selectivity towards the β-(*E*)-vinylsilane and significant amounts of alkene, from the competitive dehydrogenative silylation, has been observed. Compound **1**, unreactive towards silanes, reacts with a range of terminal alkynes RC≡CH affording unsaturated η^1-alkenyl complexes [Ir(κ^3-hqca)(*E*-CH=CHR)(coe)] in good yield. These species are able to coordinate monodentate neutral ligands as PPh_3 and pyridine, or CO in a reversible way, to yield octahedral derivatives. Further mechanistic aspects of the hydrosilylation process have been studied by DFT calculations. The catalytic cycle passes through Ir(III) species with a iridacyclopropene (η^2-vinylsilane) complex as the key intermediate. It has been found that this species may lead both to the dehydrogenative silylation products, via a β-elimination process, and to a hydrosilylation cycle. The β-elimination path has higher activation energy than the hydrosilylation. On the other hand, the selectivity to the vinylsilane hydrosilylation products can be accounted for by the different activation energies involved in the attack of a silane molecule at two different faces of the iridacyclopropene ring to give η^1-vinylsilane

complexes with either an *E* or *Z* configuration. Finally, proton transfer from a η^2-silane to the η^1-vinylsilane ligand results in the formation of the corresponding β-(*Z*) and β-(*E*)-vinylsilane isomers, respectively.

Introduction

Transition-metal catalyzed hydrosilylation of terminal alkynes is the most straightforward and atom-economical methodology for the preparation of vinylsilanes.[1] Unsaturated hydrosilylation products are valuable synthetic intermediates due to their versatility, ease of handling, low toxicity, and stability relative to other vinyl-metal species.[2] The hydrosilylation of terminal alkynes can afford several isomeric vinylsilanes and therefore, the control of the regio- and stereoselectivity of the reaction is a key issue. In general, the selectivity depends upon several factors such as the catalyst, the substituents on the hydrosilane and the alkyne, and the reaction conditions. In this context, a deeper understanding of the reaction mechanisms is pivotal for the development of more active and selective catalytic systems.[1b]

The catalytic hydrosilylation of terminal alkynes normally proceeds with *anti*-Markovnikov regiochemistry and predominantly *syn*-addition stereochemistry, which can be rationalized by the classic Chalk-Harrod mechanism.[3] This inner sphere mechanism involves the oxidative addition of the hydrosilane, followed by sequential coordination and hydrometallation of the alkyne, as the regio-determining step, and results in the predominant formation of the most thermodynamically stable β-(*E*)-vinylsilane after reductive elimination. This mechanism seems to be operative with Pt-based catalysts[4] but is unable to explain the formation of β-(*Z*)-vinylsilane, the *trans*-addition product, or silylalkyne derivatives resulting from the competitive dehydrogenative silylation process observed with Rh,[5] Ir[6,7] and Ru-based[8] catalysts.

The formation of both types of products can be explained by the modified Chalk-Harrod mechanism that entails the silyl-metallation of the alkyne by migratory insertion into the M-

Si bond to give a (*Z*)-silylvinylene metal complex.[1] The formation of the β-(*Z*)-vinylsilane requires the metal-assisted isomerization of the (*Z*)-silylvinylene intermediate to the thermodynamically more favorable (*E*)-silylvinylene complex with the relief of steric strain between the metal and the adjacent silane as the driving force of the process. This isomerization proceeds through a η^2-vinylsilane or metallacyclopropene intermediate in the mechanism proposed by Crabtree *et al.*[9] for Ir-catalyzed reactions (Scheme 1, i), or a zwitterionic carbene species in the mechanism proposed by Ojima *et al.*[10] for Rh-catalyzed processes (Scheme 1, ii). Thus, because the reductive elimination is the rate-determining step, the less thermodynamically stable β-(*Z*)-vinylsilane isomer is formed as the kinetic product. In addition, β-H elimination from (*E*)-silylvinylene intermediates affords the silylalkyne derivative and dihydrido complex which can be reduced by the alkyne giving the corresponding alkene (Scheme 1, iii).

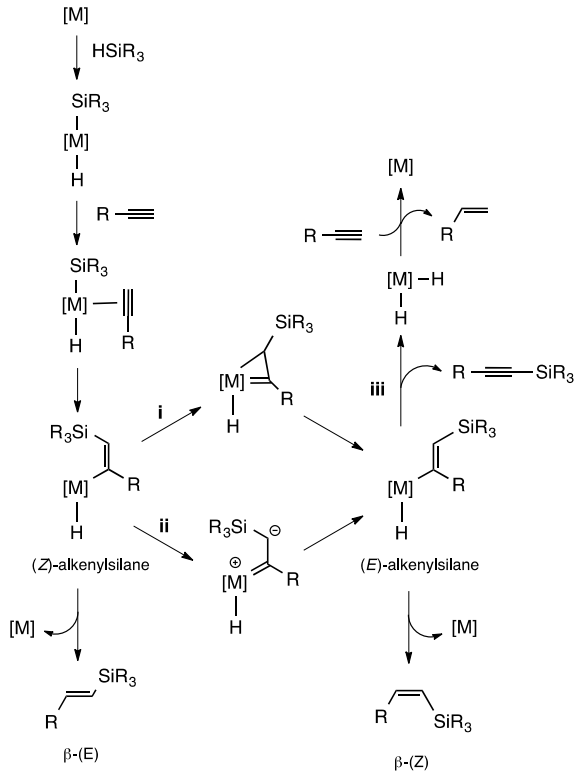

Scheme 1. The Crabtree-Ojima mechanism for alkyne hydrosilylation.

A third mechanistic proposal, the Wu-Trost mechanism, has been put forward to explain the unusual Markovnikov regioselectivity and exclusive *trans*-addition stereochemistry found in the hydrosilylation of terminal and internal alkynes by cationic cyclopentadienyl Ru^{II} catalysts.[11] The reaction proceeds through an oxidative hydrometalation step, that involves the oxidative addition of the Si-H bond concerted with hydrometallation, and result in the formation of a ruthenacyclopropene intermediate, which undergoes reductive silyl migration to the carbene affording the α-vinylsilane isomer (Scheme 2). On the other hand, we have recently proposed an outer-sphere ionic mechanism for the hydrosilylation of terminal alkynes catalyzed by mononuclear Rh^{III} and Ir^{III} catalyst precursors featuring a functionalized bis-N-heterocyclic carbene ligand. The mechanism involves the heterolytic splitting of the hydrosilane assisted by the electrophilic metal center and the solvent (acetone) resulting in the formation of an intermediate silylcarboxonium ion that transfers the silyl moiety to the alkyne resulting in outstanding β-Z selectivity.[12]

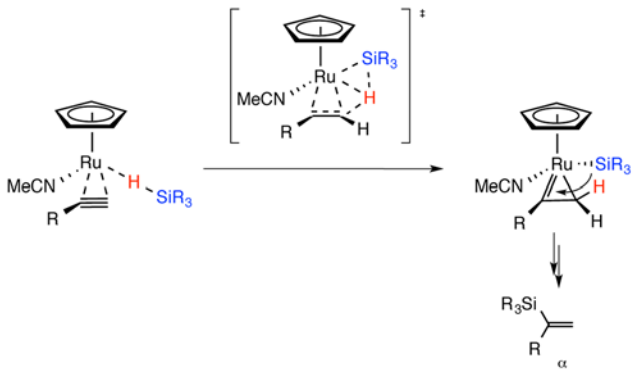

Scheme 2. Oxidative hydrometallation step in the Wu-Trost hydrosilylation mechanism leading to the formation of the α-vinylsilane isomer.

The well established modified Chalk-Harrod mechanism relies on the detection of metal intermediates by spectroscopic techniques, kinetic analysis, deuterium labeling or reactivity studies on well defined models of reaction intermediates.[13] Strong support for this mechanism also comes from the detection of key reaction intermediates by electrospray

ionization mass spectrometry (ESI-MS).[14] Interestingly, a number of computational studies on the mechanism of ruthenium-catalyzed alkyne hydrosilylation have been recently reported,[11,15] which contrast with those based on rhodium and iridium catalysts which have been mainly focused on the hydrosilylation of alkenes or carbonyl compounds.[16]

The modified Chalk-Harrod mechanism perfectly fits to a catalytic cycle passing through Pt^0/Pt^{II} or M^I/M^{III} (M = Rh, Ir) intermediates. However, in the case of iridium(III) precatalysts the possible involvement of Ir^{III}/Ir^V species as catalytic intermediates cannot be excluded. In fact, experimental and theoretical studies have provided evidence for the intermediacy of Ir^V species in iridium-catalyzed C-H activation/functionalization processes,[17] alkene hydrogenation reactions,[18] or in the outer-sphere hydrosilylation of carbonyl compounds.[19] In this context, it is worth mentioning that computational studies on the mechanism of the stereoselective hydrosilylation of terminal alkynes catalyzed by $[Cp^*IrCl_2]_2$ support an Ir(III/V) catalytic cycle assisted by the ring slippage of the Cp* ligand.[20]

Pincer ligands are valuable structural motifs for the design of transition-metal complexes for selective stoichiometric and catalytic transformations.[21] O-based anionic pincer ligands have attracted significant attention for supporting high-oxidation-state metal complexes with vacant coordination sites.[22] The robustness and stability of the ligand framework in combination with strongly electron donating hard oxygen donor atoms provide access to higher oxidation states of the metal centers by modulating the electron density at the metal via a hard/hard interaction or π-donating effects.[23] We have recently shown the potential of tridentate dianionic ONO pincer ligands for the design of unsaturated iridium(III) compounds which have shown catalytic activity in C–H activation/functionalization processes.[24,25]

We report herein on the catalytic activity of the unsaturated hydrido iridium(III) compound [IrH(κ^3-hqca)(coe)] (hqca = 8-oxidoquinoline-2-carboxylate) in the hydrosilylation of

terminal alkynes. In principle, the presence of a rigid asymmetrical dianionic ONO pincer ligand could facilitate the stabilization of Ir^V intermediates thereby driving the catalytic reaction through a Ir(III/V) mechanism. Thus, the hydrosilylation and dehydrogenative silylation mechanisms have been investigated by theoretical calculations at DFT level. In addition, a reactivity study leading to the preparation of a series of iridium(III) η^1-alkenyl complexes is also described.

Results and Discussion

The square-pyramidal iridium(III) complex [IrH(κ^3-hqca)(coe)] (**1**) was straightforwardly prepared by reaction of [Ir(μ-OH)(coe)$_2$]$_2$ with H_2hqca (8-hydroxyquinoline-2-carboxylic acid). Interestingly, compound **1** exists as dinuclear assemblies [IrH(κ^3-hqca)(coe)]$_2$ in non-coordinating solvents and as labile mononuclear solvates in polar solvent solutions. The presence of a vacant coordination site trans to the hydrido ligand in **1** allowed the preparation of several octahedral [IrH(κ^3-hqca)(coe)L] (L = py, PPh_3) complexes.[25] The presence of a hydrido ligand in **1** prompted us to study its reactivity with alkynes in spite that its stereochemistry is unsuitable for the insertion into the Ir-H bond.

Reaction of [IrH(κ^3-hqca)(coe)] (1) with terminal alkynes. Treatment of a tetrahydrofurane solution of **1** with a range of terminal alkynes RC≡CH (1:5 molar ratio) for 48 h at 298 K gave dark red solutions from which the η^1-alkenyl complexes [Ir(κ^3-hqca)(*E*-CH=CHR)(coe)] were isolated as red solids in good yields (Scheme 3). The reactions with the linear alkynes 1-hexyne or 1-octyne proceeded cleanly and the η^1-alkenyl complexes **3** and **4** were obtained in yields higher than 95%. However, complexes **2** and **5**, obtained from the reaction with the functionalized alkyne 3-methoxy-1-propyne and the bulky 3,3-dimethyl-1-butyne, respectively, required chromatographic purification and consequently were obtained in lower yield (60-70%). The complexes were fully characterized by elemental analysis, mass spectrometry and NMR spectroscopy. The MS (MALDI-Tof) spectra of the

compounds showed the molecular ion with the correct isotopic distribution and also the peaks corresponding to the loss of the alkenyl ligand. The complexes have a limited solubility in most organic solvents, including dichloromethane or methanol, although they have an acceptable solubility in a mixture of both solvents. Thus, the NMR spectra were routinely recorded in a MeOH-d_4/CD_2Cl_2 mixture. The ^{1}H NMR spectra of the complexes showed the expected set of five resonances in the range δ 8.3-6.8 ppm for the tridentate 8-oxidoquinoline-2-carboxylato ligand, which were assigned with the help of two-dimensional NMR techniques (see Experimental Section). The spectra also showed two resonances at δ 6.8-6.2 ppm (d) and 4.6-4.3 (dt, $^3J_{H\text{-}H} \approx 14$ Hz, **2**-**4**; d, **5**) ppm for the α and β protons of the η^1-alkenyl ligand, respectively. The large $^1J_{H\text{-}H}$ coupling constant of ≈ 14 Hz is in agreement with the presence of η^1-(*E*)-alkenyl ligand resulting from the anti-Markovnikov *syn*-addition of the Ir-H bond to the alkynes. The =CH protons of the η^2-cyclooctene ligand were observed as a complex multiplet centered around δ 5.12 ppm. The $^{13}C\{^1H\}$ NMR spectra are in full agreement with the unsymmetrical structure of the complexes and show a set of eight resonances for the coe ligand, two of them at around δ 88-86 ppm for the =CH carbons.

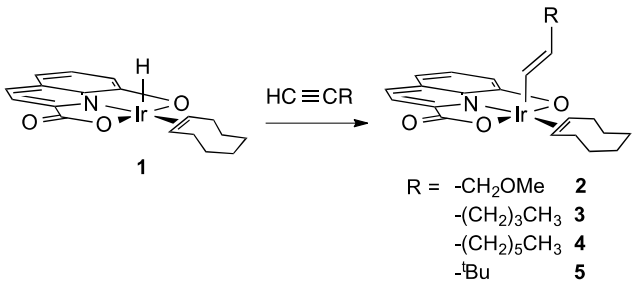

Scheme 3. Synthesis of η^1-alkenyl [Ir(κ^3-hqca)(*E*-CH=CHR)(coe)] (**2**-**5**) complexes.

The labeled complex [IrD(κ^3-hqca)(coe)] (**1**-***d*$_1$**) was prepared in situ by H/D exchange in a THF/MeOH-d_4 solution in a few minutes. Reaction of **1**-***d*$_1$** with 1-hexyne gave the deuterium labeled complex [Ir(κ^3-hqca)(*E*-CH=CD$(CH_2)_3CH_3$)(coe)] (**3**-***d*$_1$**) which was isolated as a red solid in 96% yield. The full characterization of **3**-***d*$_1$** supports the regio- and stereoselectivity

of the insertion process in **1** that proceeds in a *syn* fashion.[26] Thus, the lack of the resonance at δ 4.30 ppm in the ^{1}H NMR spectrum of **3-*d*$_1$** and the deuterium coupled triplet resonance at δ 133.46 ppm ($^1J_{C\text{-}D}$ = 26.6 Hz) confirms the deuterium incorporation at the β carbon of the alkenyl ligand.

The alkyne insertion reaction in **1** has been studied by DFT calculations using CH_3-C≡CH as alkyne model. Coordination of propyne to give the octahedral complex **1-alky**, which has an alkyne molecule in a relative cis position to the hydrido ligand, is -7.0 kcal/mol downhill. The insertion of propyne into de Ir-H bond to give the η^1-alkenyl complex [Ir(κ^3-hqca)(*E*-CH=CHCH$_3$)(coe)] (**6**) is calculated to be further downhill by -7.6 kcal/mol and requires an activation energy of 21 kcal/mol, which is affordable at room temperature (Scheme 4).

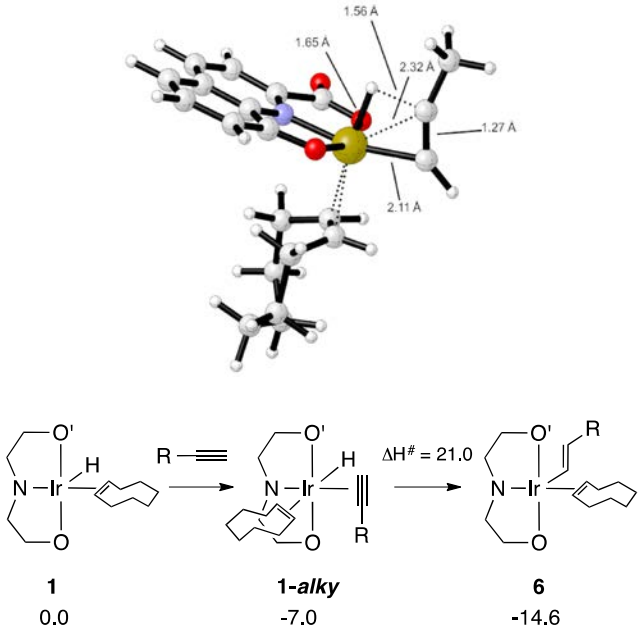

Scheme 4. Computed energies (ΔH, Kcal/mol) for the insertion of propyne into the Ir-H bond of **1** (ONO' = 8-oxidoquinoline-2-carboxylato) and structure of the **TS$_{1\text{-}alky\text{-}6}$** (at the top).

In compound **1-alky** the propyne ligand lies parallel to the ONO plane. Due to the asymmetry of this ligand two orientations of the alkyne ligand are possible but DFT calculations show that they differ in just 0.1 kcal/mol and thus, only one of the insertion paths has been studied. In the transition structure from **1** to the insertion derivative **6** the propyne

ligand rotates and positions perpendicular to ONO plane and parallel to the Ir-H bond (Scheme 4). The Ir-H elongates to 1.65 Å in the TS from 1.54 Å in compound **1-alky**. The propyne ligand loses linearity in the process of changing its coordination mode for π-alkyne to σ-alkenyl and, consequently, the C-C-C bond angle changes from 163.3º in **1-alky** to 154.1º in the TS, and the C-C-H to 139.1º from 167.0º.

The insertion of internal alkynes into the Ir-H bond of **1** proceeds with the same selectivity as it has been demonstrated in the reaction with 2-butyne. However, the formation of the expected compound [Ir(κ^3-hqca)(*E*-(CH_3)C=$CHCH_3$)(coe)] is accompanied by a second species (20%) that could not be separated by chromatography. Likely, this minor species results from the isomerization of the alkenyl ligand although we have not yet been able to fully characterize this species by NMR.

Reactivity of [Ir(κ^3-hqca)(*E*-CH=CHCH$_2$OMe)(coe)] (2). The unsaturated complexes [Ir(κ^3-hqca)(*E*-CH=CHR)(coe)] feature a vacant site trans to the alkenyl ligand that makes possible the preparation of octahedral complex by reaction with monodentate neutral ligands. Reaction of **2** with triphenylphosphine at room temperature cleanly gave the octahedral adduct [Ir(κ^3-hqca)(*E*-CH=$CHCH_2OMe$)(coe)(PPh_3)] (**2-PPh$_3$**) which was isolated as a yellow solid in 69 % yield (Scheme 5). The coordination of the PPh_3 ligand became evident in the $^{31}P\{^1H\}$ NMR that features a singlet at δ -11.25. The α carbon of the η^1-alkenyl ligand appears as a doublet at δ 138.13 ppm with a large $^2J_{C\text{-}P}$ = 113.6 Hz coupling constant in the $^{13}C\{^1H\}$ NMR spectrum which support the coordination of the PPh_3 ligand trans to the alkenyl ligand. In addition, the α and β vinyl protons were observed at δ 6.79 and 4.74 ppm in the ^1H NMR as dd and ddt due to the long range coupling to the phosphorous atom with $^3J_{H\text{-}P}$ and $^4J_{H\text{-}P}$ coupling constants of 6.8 and 8.0 Hz, respectively. The presence of the coe ligand in **2-PPh$_3$** was confirmed both in the ^1H and $^{13}C\{^1H\}$ NMR spectra which showed two

resonances for the =CH protons and carbons at δ 5.40 and 5.20 ppm, and 85.85 and 85.40 ppm, respectively.

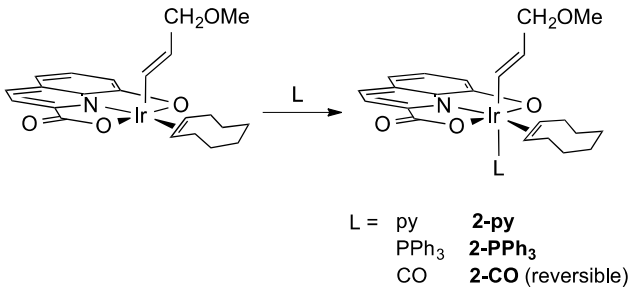

Scheme 5. Reactivity of [Ir(κ^3-hqca)(*E*-CH=CHCH$_2$OMe)(coe)] (**2**).

The adduct [Ir(κ^3-hqca)(*E*-CH=CHCH$_2$OMe)(coe)(py)] (**2-py**) was prepared by reaction of **2** with an excess of pyridine and isolated as an orange solid in excellent yield. The stereochemistry of **2-py** was unequivocally established by means of the ^{1}H-^{1}H NOESY spectrum that showed cross peaks between the *ortho* pyridine protons and the nearest >CH$_2$ protons of the coe ligand, and between the α proton of the η^1-alkenyl ligand and the =CH coe protons. Thus, the alkenyl and pyridine ligands in **2-py** are mutually *trans* disposed thereby confirming that py occupies the vacant position in **2** (Scheme 5).

The carbonylation of a solution of **2** in dichloromethane/methanol for 1 hour at room temperature resulted in the formation of the carbonyl complex [Ir(κ^3-hqca)(*E*-CH=CHCH$_2$OMe)(coe)(CO)] (**2-CO**) which is in equilibrium with **2** (40:60 ratio, NMR evidence). The formation of **2-CO** is supported by the IR spectrum that features a strong absorption at 2035 cm^{-1} corresponding to the terminal carbonyl stretching ν(CO) band. The carbonylation of **2** is reversible and in fact, all the attempts to isolated **2-CO** in the solid state resulted in the crystallization of **2**.

Hydrosilylation of 1-alkynes. Complex [IrH(κ^3-hqca)(coe)] (**1**) was found to be an efficient catalyst precursor for the hydrosilylation of terminal alkynes. The catalytic reactions were performed in CDCl$_3$ at 60 ^{o}C using a 2 mol% catalyst loading and a slight excess of

hydrosilane, and routinely monitored by ^{1}H NMR spectroscopy. A range of aliphatic and aromatic 1-alkynes was efficiently reduced in approximately one hour using $HSiMePh_2$, $HSiMe_2Ph$ and $HSiEt_3$ as hydrosilanes (Table 1). Hydrosilylation of terminal alkynes can result in three isomeric vinylsilane derivatives: (*Z*)- or (*E*)-1-silyl-1-alkenes, products from the anti- Markovnikov addition, namely β-(*Z*) and β-(*E*)-vinylsilane isomers, respectively; and 2-silyl-1-alkene from the Markovnikov addition (α isomer). In addition, the formation of the dehydrogenative silylation products, alkynylsilane and the corresponding alkene, has been observed to some extent particularly in the case of sterically demanding substituents on the alkyne and/or the hydrosilane (Scheme 6).

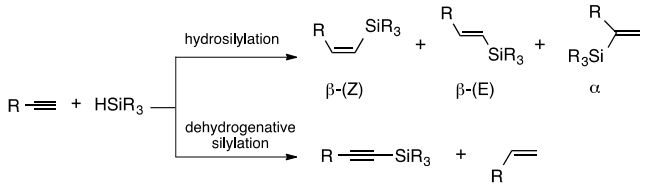

Scheme 6. Hydrosilylation and dehydrogenative silylation of terminal alkynes.

Table 1. Hydrosilylation of terminal alkynes with 8-oxidoquinoline-2-carboxylato iridium(III) complexes.[a, b]

entry	catalyst	R-C≡CH (R)	silane	time (h)	conv. (%)	β-(*Z*) (%)	β-(*E*) (%)	α (%)	alkene (%)
1	**1**	*n*-Bu	$HSiMePh_2$	1	100	88	8	0	4
2	**3**		$HSiMePh_2$	1	100	91	7	0	2
3	**1**		$HSiMe_2Ph$	0.75	100	83	14	0	3
4	**1**		$HSiEt_3$	0.75	100	68	21	8	3
5	**3**		$HSiEt_3$	0.75	100	62	28	8	2
6	**1**	*n*-Hex	$HSiMePh_2$	1	100	83	8	3	6
7	**1**		$HSiMe_2Ph$	0.75	100	72	20	0	8
8	**1**		$HSiEt_3$	0.5	100	70	13	7	10

9	**1**	*t*-Bu	$HSiMePh_2$	1	56	13	51	5	31
10	**1**		$HSiEt_3$	0.5	100	9	58	3	30
11	**1**		$HSiEt_3$	2 [c]	59	9	57	4	30
12	**1**	$SiEt_3$	$HSiMePh_2$	1	17	82	10	0	8
13	**1**		$HSiEt_3$	1.3	87	94	3	0	3
14	**1**	Ph	$HSiMePh_2$	1	100	45	37	9	9
15	**1**		$HSiEt_3$	0.2	100	71	18	6	5
16	**1**		$HSiEt_3$	0.5	100	63	25	6	6
17	**1**	4-MeO-C_6H_4	$HSiMePh_2$	1	100	29	66	2	3
18	**1**		$HSiEt_3$	0.15	100	80	11	5	4
19	**1**		$HSiEt_3$	1.15	100	43	50	5	2
20	**1**		$HSiEt_3$	1.5 [c]	100	87	9	2	2
21	**1**	4-CF_3-C_6H_4	$HSiMePh_2$	2.5	90	40	40	9	11
22	**1**		$HSiEt_3$	0.5	98	44	27	16	13

[a] Conversion and selectivities were calculated by ^{1}H NMR. [b] Experiments were carried out in $CDCl_3$ at 60 ^{o}C using a $HSiR_3$/RC≡CH/Ir ratio of 110/100/2, [Ir] = 3.08 mM. [c] Room temperature.

The hydrosilylation of hex-1-yne with $HSiMePh_2$ catalyzed by **1** was completed in one hour giving an 88 % of selectivity in β-(*Z*)-vinylsilane (entry 1). The reactions with $HSiMe_2Ph$ and $HSiEt_3$ are even faster, with β-(*Z*) selectivities of 83% and 68%, respectively (entries 3 and 4). The reaction profile of conversion and selectivity versus time for the hydrosilylation of hex-1-yne with $HSiMePh_2$ catalyzed by **1** is shown in Figure 1. A steady increase in the amount of β-(*E*)-vinylsilane and alkene can be seen from the beginning of the reaction reaching an 8% and 4%, respectively, after the complete conversion of the alkyne. Interestingly, the η^1-alkenyl complex [Ir(κ^3-hqca)(*E*-CH=CH$(CH_2)_3CH_3$)(coe)] (**3**) exhibited a similar catalytic performance, both in terms of activity and selectivity, compared to that of

hydrido complex **1** (entries 2 and 5) and then, catalyst **1** was used throughout the catalytic study.

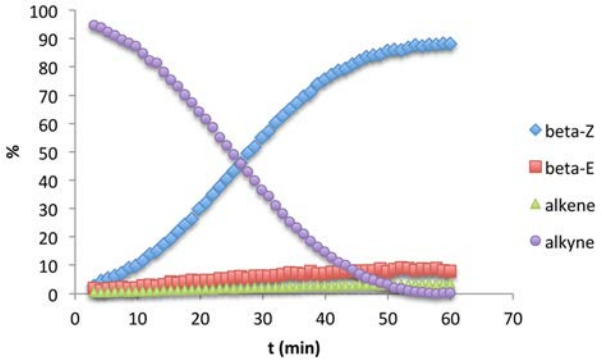

Figure 1. Reaction profile of conversion and selectivity versus time for the hydrosilylation of *n*-BuC≡CH with $HSiMePh_2$ catalyzed by **1** in $CDCl_3$ at 60 °C: β-(*Z*)-vinylsilane (❶), β-(*E*)-vinylsilane (⑤), 1-hexene (⑩), *n*-BuC≡CH (③).

Hydrosilylation of oct-1-yne showed comparable results as moderate to good selectivity to β-(*Z*)-vinylsilane was attained albeit with a slight increase in the amount of the alkene product (entries 6-8). Interestingly, the reaction with $HSiEt_3$ was completed in only 30 min with a β-(*Z*) selectivity of 70% (entry 8). However, a reverse selectivity towards the β-(*E*)-vinylsilane and a significant amount of alkene (up to 30%) was observed when using the bulky *t*-Bu-C≡CH as substrate, which follows the trend observed with rhodium(I) catalysts having alkylamino-functionalized NHC ligands.[5c] In the particular case of $HSiMePh_2$, the reaction is slower than with linear long alkyl chain alkynes giving a 56% of conversion after 1 hour (entry 9). The hydrosilylation of *t*-Bu-C≡CH with $HSiEt_3$ was performed at room temperature giving a 60% of conversion in 2 hours with the same selectivity (entries 10 and 11). In sharp contrast, excellent regio- and stereoselectivity towards the β-(*Z*)-vinylsilane was attained with the substrate Et_3Si-C≡CH. Although the reaction with $HSiMePh_2$ is much slower with only a 17% of conversion in 1 hour, $HSiEt_3$ provided the best catalytic

performance with a 94% of selectivity and 87% of conversion in only 1.3 h (entries 12 and 13).

The hydrosilylation of phenylacetylene proceeds with moderate selectivity towards the β-(*Z*)-vinylsilane isomer (entries 14 and 15). Remarkably, the formation of polyphenylacetylene was not observed, which contrasts with some rhodium(I) hydrosilylation catalysts that also promote the polymerization of substituted aromatic alkynes. [5c,27] As can be observed in the selected reaction profiles of Figure 2, the hydrosilylation of phenylacetylene with $HSiEt_3$ is faster than that of the aliphatic alkynes hex-1-yne or triethylsilyl acetylene. Also, the hydrosilylation reactions with $HSiEt_3$ are faster than with $HSiMePh_2$ as is exemplified in the case of hex-1-yne in Figure 2.

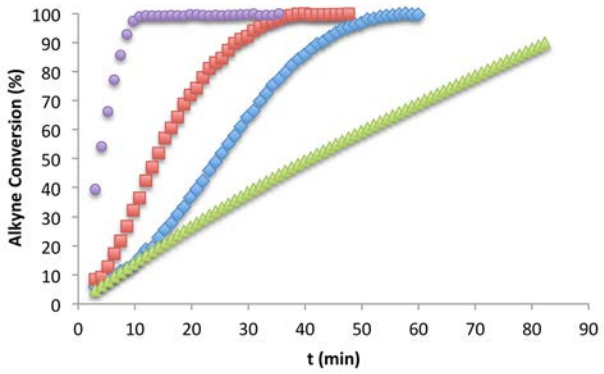

Figure 2. Reaction profile of conversion versus time for the hydrosilylation of PhC≡CH (③), *n*-BuC≡CH (⑤) and Et_3SiC≡CH (⑩) with $HSiEt_3$; and *n*-BuC≡CH (❶) with $HSiMePh_2$, catalyzed by **1** in $CDCl_3$ at 60 °C.

The selectivity in the hydrosilylation of alkynes is also influenced by the catalyst ability to promote isomerization reactions once the alkyne substrate has been completely consumed. Both the isomerization of β-(*Z*)-vinylsilane to the more thermodynamically stable β-(*E*)-vinylsilane isomer or to the corresponding allyl-silyl derivatives, in the case of linear alkyl chain alkynes, have been frequently observed.[5b-c,6e] Although catalyst precursor **1** has shown

no substantial isomerization activity for aliphatic alkynes at reasonable reactions times after the consumption of the substrate, β-(*Z*)→β-(*E*) vinylsilane isomerization process strongly determines the observed selectivity in the case of aromatic alkynes. The monitoring of the hydrosilylation of phenylacetylene with $HSiEt_3$ showed that the reaction was completed in 12 min with a 71% of selectivity to β-(*Z*)-vinylsilane. However, after 30 min the selectivity dropped to 63% as a consequence of the β-(*Z*)→β-(*E*) vinylsilane isomerization (entries 15 and 16). In agreement with these results, we have found that compound **1** efficiently promotes the isomerization of (*Z*)-PhCH=CHSiMe_2Ph into the (*E*)-vinylsilane isomer under the same experimental conditions giving a 90% of conversion in 3 hours (see Supporting Information).

The influence of the electronic effects on the hydrosilylation of alkynes has been studied with the alkynes 4'-methoxyphenyl and 4'-trifluoromethylphenyl acetylene. As can be seen in Table 1, the hydrosilylation of the phenylacetylene derivative with a -CF_3 electron-withdrawing substituent in para position is slower than that of phenylacetylene giving also poor selectivity (entries 21 and 22). Although a preference for the β-(*Z*)-vinylsilane isomer was also observed (40-44%), significant amounts of α-vinylsilane (up to 16%) and the corresponding alkene (11-13%) were produced. In order to confirm the formation of the corresponding silylalkyne derivative resulting from the competitive dehydrogenative silylation, which is difficult to identify in the ^{1}H NMR spectrum of the reaction mixture, the outcome of the hydrosilylation of 4'-trifluoromethylphenyl acetylene with $HSiEt_3$ was studied by $^{29}Si\{^{1}H\}$ NMR spectroscopy. The spectrum showed three resonances at δ 5.84, 3.29 and 1.02 ppm which were assigned to the α, β-(*E*) and β-(*Z*)-vinylsilane isomers, respectively, with the help of the ^{1}H-^{29}Si HMBC NMR correlation spectrum. The resonance at δ -3.57 ppm, which showed correlation exclusively with the ethyl resonances of the silane moiety, was assigned to the silylalkyne derivative. Furthermore, both the silylalkyne

derivative and the corresponding alkene, but no the dehydrodimerization Et_3Si-$SiEt_3$ product, were detected by GC/MS (see Supporting Information).

The presence of a -OMe electron-donating substituent in para position resulted in an increase of the activity. The hydrosilylation of 4'-methoxyphenyl acetylene with $HSiMePh_2$ gave a 66% of β-(*E*)-vinylsilane isomer with a β-(*Z*)/β-(*E*) ratio of 0.44 likely as a result of the β-(*Z*)→β-(*E*) vinylsilane isomerization after the end of the hydrosilylation reaction (entry 17). The monitoring of the reaction of 4'-methoxyphenyl acetylene with $HSiEt_3$ evidenced complete conversion in 0.15 h giving an 80% of β-(*Z*)-vinylsilane with a β-(*Z*)/β-(*E*) ratio of 7.3 (entry 18). However, this ratio steadily dropped to 0.9 after 1.15 h due to β-(*Z*)→β-(*E*) vinylsilane isomerization (entry 19 and Figure 3). Interestingly, when the hydrosilylation was performed at room temperature complete conversion was attained in only 1.5 h with 87% of β-(*Z*)-vinylsilane and a β-(*Z*)/β-(*E*) ratio as high as 9.6 (entry 20).

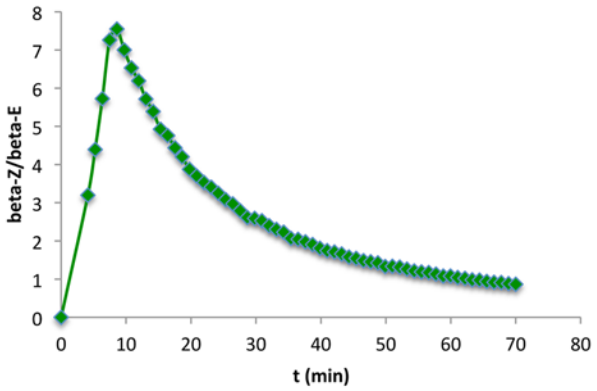

Figure 3. β-(*Z*)/β-(*E*) ratio for the hydrosilylation of 4-MeO-C_6H_4-C≡CH with $HSiEt_3$ catalyzed by **1** in $CDCl_3$ at 60 °C. Total consumption of 4-MeO-C_6H_4-C≡CH at 9 min.

The reactivity trend observed with catalyst **1** contrasts with that of some ruthenium catalysts in which electron-withdrawing substituents increased phenylacetylene reactivity toward hydrosilylation.[28] On the other hand, no major effects arising from the electronic effects of para substitution of phenylacetylenes, neither in the activity nor in the selectivity,

were found in catalytic systems based on Rh^{III} and Ir^{III} catalyst precursors featuring a functionalized bis-N-heterocyclic carbene ligand.[6,12]

Mechanism of the hydrosilylation of 1-alkynes catalyzed by [IrH(κ^3-hqca)(coe)] (1). Compound **1** does not react with hydrosilanes such as $HSiMePh_2$ or $HSiEt_3$ in $CHCl_3$ at 60 ^oC. Thus, the η^1-alkenyl complexes [Ir(κ^3-hqca)(*E*-CH=CHR)(coe)] formed in the reaction of **1** with terminal alkynes should play a key role in the mechanism of the hydrosilylation of terminal alkynes. According to these experimental observations, the catalytic reaction should start by reaction of the alkenyl species with hydrosilane.

In order to shed light on the reaction mechanism, a computational study at the DFT level has been carried out using $HSiMe_3$ as a model for silanes and propyne as an alkyne model. A double catalytic cycle based on Crabtree's proposal has been studied.[6e] The proposed mechanism for the hydrosilylation and dehydrogenative silylation of terminal alkynes catalyzed by **1** is shown in Scheme 7. In the following discussion all the energies are reported in terms of ΔH. One of the key steps in the process is the competitive reaction of intermediate **10** in an unimolecular β-H elimination process, to follow a reductive silylation path through intermediate **13**, or an alternative bimolecular reaction with a silane molecule to a silylation process through **11** (Scheme 7). A bimolecular process suffers of a penalty because of the overestimation of entropy in the Gibbs energy calculations favoring the unimolecular process. While some approximate corrections have been proposed, we think that ΔH reproduces sufficiently the observed experimental trends and will be used through the whole discussion.[29] Full data (electronic energy, enthalpy and free energies in gas phase) for every intervening molecule or transition state, are included in the Supporting Information.

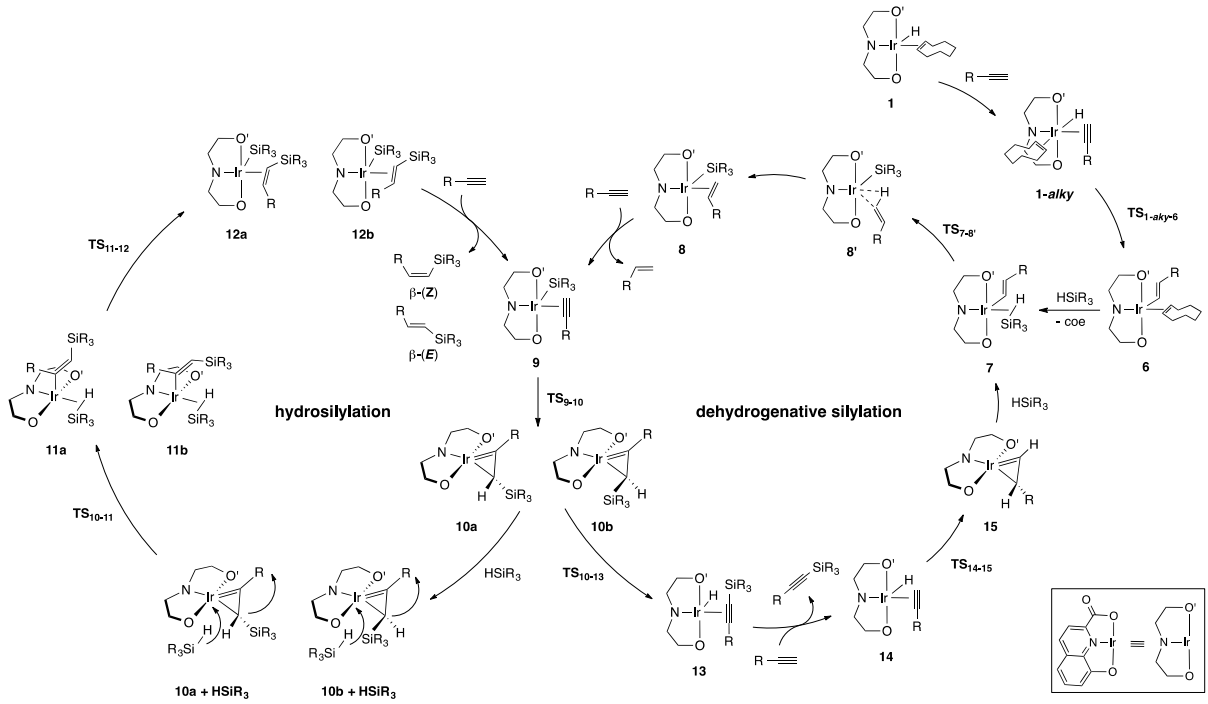

Scheme 7. Proposed mechanism for the hydrosilylation (left) and dehydrogenative silylation (right) of terminal alkynes catalyzed by **1**.

The reaction of **6** with $HSiMe_3$ displaces the coe ligand from the metal coordination sphere in an exothermic step (ΔH = -8.3 kcal/mol) to give **7**, which then starts the catalytic cycle (Scheme 7). This is a η^2-silane compound which leads to the formation of propene by σ-bond Si-H metathesis via $\mathbf{TS_{7\text{-}8'}}$ ($\Delta H^{\#}$ = +4.8 kcal/mol) (Figure 4). An intrinsic reaction coordinate (IRC) calculation from the transition state produces a η^2-alkene agostic complex **8'** which eventually rearranges to a more stable π-coordinated alkene complex **8**. This step is exothermic from **7** releasing ΔH = -30.3 kcal mol^{-1}. Interestingly, no intermediate corresponding to an oxidative addition of silane to yield an Ir(V) species has been found. As shown in Figure 4, the Ir-H distance in $\mathbf{TS_{7\text{-}8'}}$ is 1.60 Å, while the Si-H (2.05 Å) and the C-H (1.99 Å) bond distances are both long. These data suggest that the breaking Si-H bond is quite advanced while the C-H bond is not completely formed in the transition state. In addition, the Ir-H bond has a considerable hydridic character, which is compatible with a hydrogen transfer step occurring via an oxidative hydrogen migration mechanism.[11a,15a]

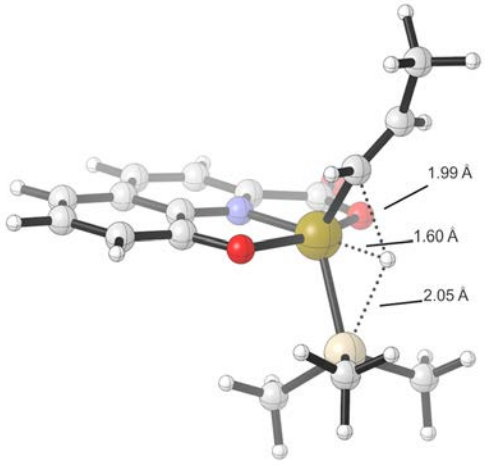

Figure 4. Structure of $\mathbf{TS_{7\text{-}8}}$, with some relevant bond distances.

Substitution of the alkene ligand in **8** by propyne is favoured (ΔH = -3.9 kcal mol^{-1}) and gives complex **9** with a square pyramidal geometry. In this complex the ONO pincer ligand and the alkyne are coplanar while the silyl group is located at the apical vertex of the pyramid. Due to the asymmetry of the ONO ligand, two possible orientations of the alkyne molecule are possible although the difference in stability between them (**9a** and **9b**) is quite small, just 0.3 kcal mol^{-1}. After this step the reaction pathway splits into the two separated hydrosilylation and dehydrogenative silylation cycles (Scheme 7). This common intermediate to both cycles is shown as origin and reference in the energy profile for the hydrosilylation cycle shown in Figure 5.

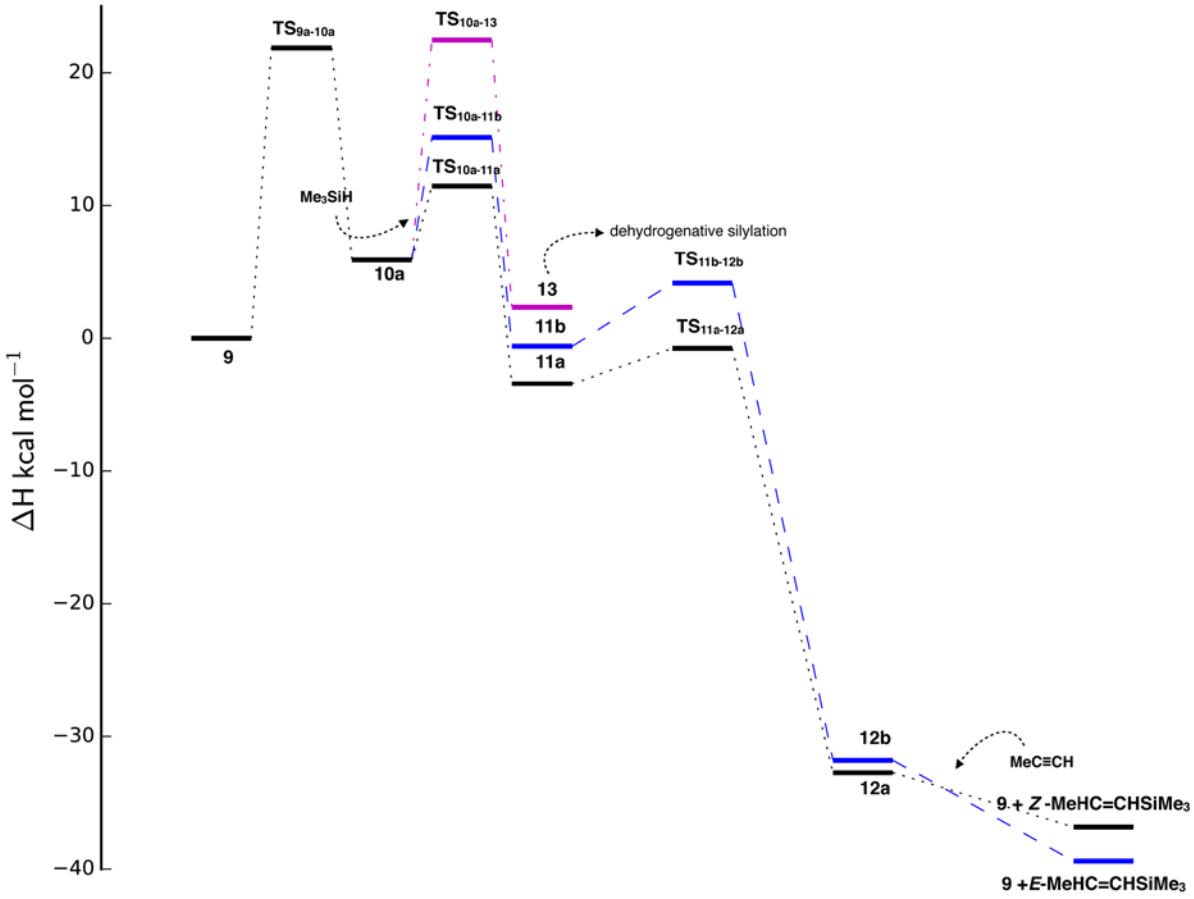

Figure 5. Energy profile for the hydrosilylation cycle (Scheme 7, left). **TS_{10a-13}** and **13** lead to the dehydrogenative silylation pathway that has been omitted for clarity (both energy profiles are shown together in the Supporting Information). **9** has been chosen as starting compound for the diagram as it is the common point between both cyclic processes.

The silyl group in **9** migrates to the α carbon of the alkyne ligand. Due the asymmetry of the ONO pincer ligand two TSs are possible although, as it has been shown above, the energy difference between both TSs is negligible (ΔH = 0.25 kcal/mol) with an energy difference of ΔH = 0.2 kcal/mol between both possible isomer products, **10a** and **10b**, resulting from the location of the silyl substituent relative to the two different functional groups of the ONO pincer ligand (Figure 6). The activation energy for this process is $\Delta H^{\#}$ = +21.6 kcal/mol from **9a** to **10a**. The compounds **10a** and **10b**, that feature a η^2-vinylsilane ligand perpendicular to the ONO plane, are endothermic relative to **9a** or **9b** by ca. 6.0 kcal/mol. Interestingly, η^2-

vinylsilane metal species, also named metallacyclopropene complexes, have been proposed as a key intermediates in several hydrosilylation mechanisms.[11b, 30, 31a]

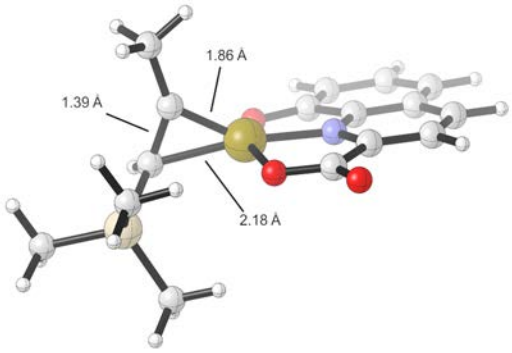

Figure 6. Structure of one of the isomers of the η^2-vinylsilane compound **10**.

In the next step, an $HSiMe_3$ molecule enters in the coordination sphere of the iridium center by bonding in a η^2 fashion while the η^2-vinylsilane ring opens by breaking the Ir-Cα bond and rotates around the Ir-Cβ bond producing an ensuing η^1-vinylsilane ligand. This step is the origin of the stereoselectivity of the global reaction as the approach of the $HSiMe_3$ can take two pathways relative to the substituents on the Cα atom (Scheme 7). This leads to two different TSs for each isomer of **10**, which eventually produce two square pyramidal complexes, **11a** and **11b**, where the final η^1-vinylsilane ligand has either a *Z* or *E* configuration, respectively. A total of four transition structures are then possible. As stated above the different orientations relative to the ONO ligand are, in practice, irrelevant. Those two leading to a (*Z*)-silylvinylene ligand are the most feasible with an activation energy of $\Delta H^{\#}$ = +5.6 kcal/mol, the difference between both of them being 0.4 kcal/mol. Those which will yield a (*E*)-silylvinylene compound are ca. 3 kcal/mol higher in energy with an activation energy of $\Delta H^{\#} \approx$ +8 kcal/mol. During this process the C-C distance varies form 1.39 Å in the η^2-vinyl complex to 1.35 Å in the TSs, and reach a value of 1.34 Å in the final η^1-vinyl complexes **11**, with small differences in the third decimal place for both isomers. More significant is the change in the Ir-C distances, which starts at a value of 1.86 Å in both

isomers of **10** and ends at a value of 2.04 Å in **11**, reflecting a significant change in the metal-carbon bond order, with an intermediate value of 1.94 Å in the TS.

Formation of **11a** is exothermic relative to **10a** (ΔH = -9.3 kcal/mol) while **11b** is exothermic by a slightly lesser amount (ΔH = -6.5 kcal/mol). A more favorable transition state and a slightly greater stability of the final intermediate complex drive the process towards the formation of the (*Z*)-silylvinylene iridium derivative. The steric interaction between the entering silane molecule and the silyl substituent is at the origin of this difference. The entrance of the $HSiMe_3$ molecule in the iridium coordination sphere, by any of the two planes of the metallacyclopropene moiety, moves away from it the closest substituent on the η^2-vinylsilane moiety while the rotation around the C-C approaches the second substituent to the entering silane. In this way, attack from the H side of the η^2-vinylsilane rotates the H atom away from the entering silane but then approaches the silyl substituent to it. This approach would yield ultimately the β-(*E*)-vinylsilane isomer (Scheme 8, left). An attack from the opposite side reliefs any steric repulsion between the entering silane molecule and the silyl substituent making the formation of the β-(*Z*)-vinylsilane isomer much easier than the β-(*E*) counterpart (Scheme 8, right).

The η^2-$HSiMe_3$ ligand transfers the H atom to the η^1-vinylsilane ligand in an easy σ-bond Si-H metathesis process resulting in the formation of the η^2-coordinated vinylsilane products **12a** and **12b** (Scheme 7). Attempts to optimize Ir(V) structures that would correspond to an hypothetical oxidative addition of $HSiMe_3$ have been unsuccessful. In a similar fashion to that described above for $\mathbf{TS_{7\text{-}8'}}$, the process occurs via an oxidative hydrogen migration mechanism. Activation energy from **11a** to **12a** is $\Delta H^{\#}$ = +2.7 kcal/mol and from **11b** to **12b** $\Delta H^{\#}$ = + 4.7 kcal/mol. The final η^2-vinylsilane products are both of similar energy (there is a

difference of just 0.2 kcal/mol). The replacement of the formed η^2-vinylsilane ligand by a new molecule of alkyne starts a new catalytic cycle.

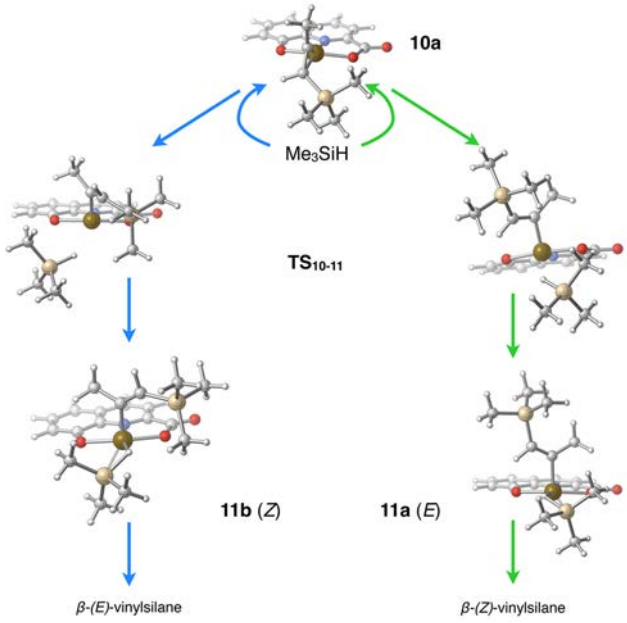

Scheme 8. Reaction of **10a** with $HSiMe_3$ to give β-(*E*) (left) or β-(*Z*)-vinylsilane (right) isomers.

The silylpropyne product resulting from the competitive dehydrogenative silylation process can be formed by β-H elimination from the η^2-vinylsilane ligand in compounds **10a** or **10b** (Scheme 7). Passing through $\mathbf{TS_{10a\text{-}13}}$ involves a relatively low activation energy of $\Delta H^{\#}$ = +16.6 kcal/mol (Figure 7) but larger than those of the hydrosilylation steps (around 5 to 8 kcal/mol, depending on isomer). The process is slightly exothermic (ΔH = -3.6 kcal/mol) and generates a hydrido silylalkyne complex **13** (only one isomer has been considered), which on replacement of the silylpropyne moiety for propyne generates **14**. Then, insertion of the alkyne into the Ir-H bond ($\Delta H^{\#}$ = 22.7 kcal/mol) yields **15**, a η^2-vinyl complex, by a slightly endothermic process (ΔH = +3.4 kcal/mol). The opening of the iridacyclopropene moiety in **15** by coordination of a silane molecule to give **7**, which restart the catalytic cycle, is an exothermic process (ΔH = -22.4 kcal/mol).

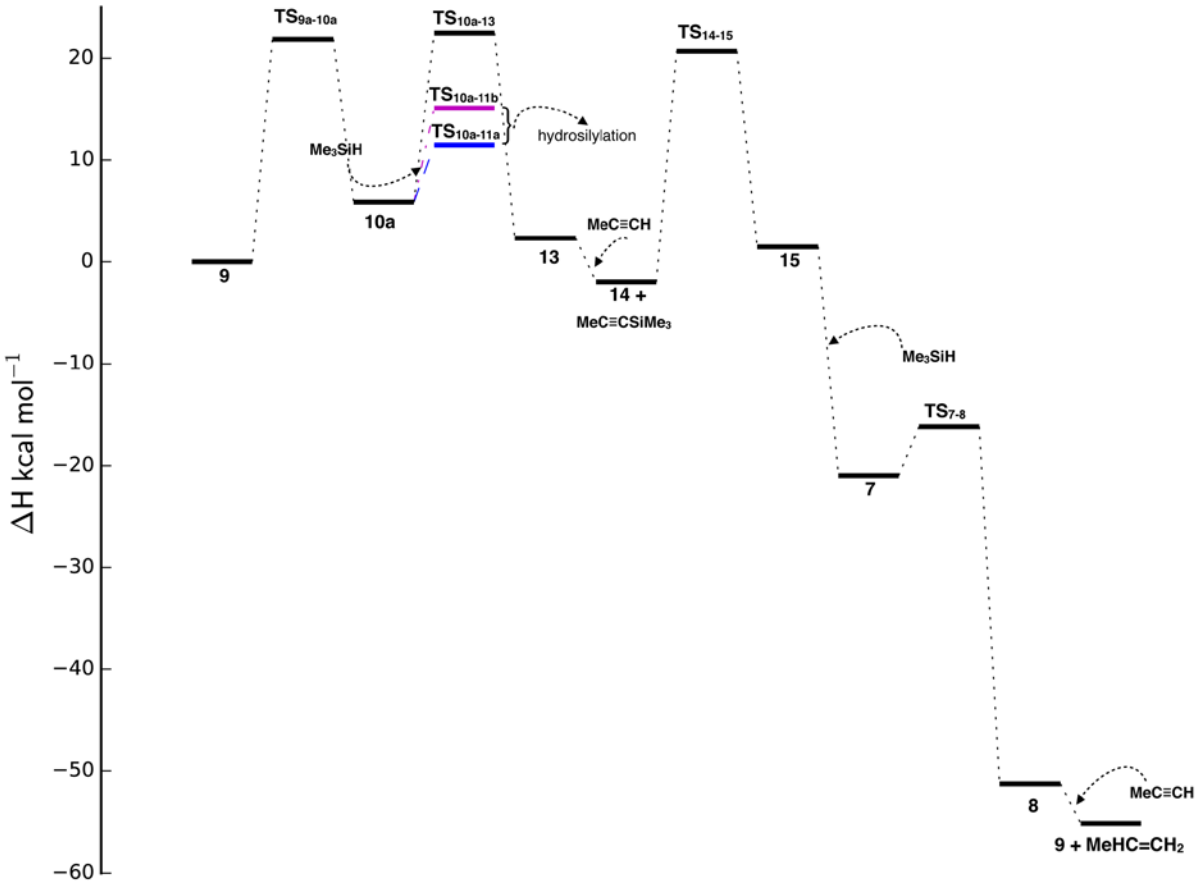

Figure 7. Energy profile for the dehydrogenative silylation cycle (Scheme 7, right). **$TS_{10a\text{-}11b}$** and **$TS_{10a\text{-}11a}$** lead to the hydrosilylation pathway that has been omitted for clarity (both energy profiles are shown together in the Supporting Information). **9** has been chosen as starting compound for the diagram as it is the common point between both cyclic processes.

The above-described mechanism helps to explain some of the trends observed in the catalytic performance of **1**. In general, good selectivity to the β-(*Z*)-vinylsilane product is achieved in the hydrosilylation of linear 1-alkynes such as hex-1-yne or oct-1-yne. However, the attained selectivity drops when decreasing the size of the hydrosilane $HSiMePh_2$ > $HSiMe_2Ph$ > $HSiEt_3$ (Table 1). As can be seen in the transition state leading to the intermediate **11b** from **10a** (Scheme 7, right), the silyl fragment of the η^1-vinylsilane ligand is directed away from the plane defined by the ONO pincer ligand also avoiding the steric clash with the entering hydrosilane. Thus, increasing the size of the silane makes this

pathway, leading to the β-(*Z*)-vinylsilane product, more competitive. However, the steric influence of the alkyne substituent must also be taken in consideration because the substituent of the alkyne is directed towards the plane of the ONO ligand after the opening of the metallacyclopropene intermediate. Then, increasing the bulkiness of the alkyne substituent introduces additional steric effects that strongly influences the β-(*Z*)/β-(*E*) ratio. As a larger substituent is subject to a greater steric repulsion with the ONO ligand, the hydrosilylation process becomes less favorable respect to the β-H elimination which results in an increasing amount of the dehydrogenative silylation products (R = *t*-Bu, Table 1).

Conclusions

Compound [IrH(κ^3-hqca)(coe)] (**1**), which contains the rigid asymmetrical dianionic ONO pincer-type ligand 8-oxidoquinoline-2-carboxylate, reacts with terminal alkynes to yield a series of η^1-alkenyl complexes [Ir(κ^3-hqca)(*E*-CH=CHR)(coe)]. The alkyne insertion into the Ir-H bond proceeds in a *syn* fashion as shown by the deuterium incorporation at the β carbon of the alkenyl ligand from the deuterium labeled compound [IrD(κ^3-hqca)(coe)]. The vacant coordination site at the unsaturated complex [Ir(κ^3-hqca)(*E*-CH=CHCH$_2$OMe)(coe)] can be occupied by monodentate neutral ligands such as PPh_3 or pyridine, while CO binds reversibly.

Compound [IrH(κ^3-hqca)(coe)] (**1**) is an efficient catalyst precursor for the hydrosilylation of a range of aliphatic and aromatic 1-alkynes. Hydrosilylation of linear 1-alkynes (hex-1-yne or oct-1-yne) gives a good selectivity towards the β-(*Z*)-vinylsilane product while for the bulkier *t*-Bu-C≡CH a reverse selectivity towards the β-(E)-vinylsilane and significant amounts of alkene, from the competitive dehydrogenative silylation, have been observed. The selectivity in the hydrosilylation of alkynes is also influenced by the catalyst ability to promote the vinylsilane isomerization. Although no substantial isomerization activity has

been found for aliphatic alkynes at reasonable reactions times after the consumption of the substrate, the β-(Z)→β-(E) vinylsilane isomerization strongly determines the observed selectivity in the case of aromatic alkynes.

The mechanism of the hydrosilylation process has been studied by DFT calculations. The catalytic cycle, based on Crabtree's proposal, passes through Ir(III) intermediates and splits into two different cycles leading to hydrosilylation or dehydrogenative silylation having two common intermediates. The key intermediate is a η^2-vinylsilane complex resulting from the silyl migration to the alkyne in a Ir(III)-silyl species having a η^2-alkyne ligand. This intermediate, via a high-energy β-H elimination process, may yield the dehydrogenative silylation products. Alternatively, reaction of the η^2-vinylsilane complex with silanes is an easier pathway. Coordination of a silane molecule causes the opening of the metallacyclopropene and is the origin of the selectivity between the (*Z*)- or (*E*)-1-silyl-1-alkenes products, β-(*Z*) and β-(*E*) isomers, respectively. The attack of silane onto the two different faces of the iridacyclopropene ring has a slightly different activation energy which gives raise to different η^1-vinylsilane ligands with either an *E* or *Z* configuration. σ-bond Si-H metathesis results in the H transfer from the silane to the η^1-vinylsilane ligand and the formation of the corresponding β-(*Z*) and β-(*E*)-vinylsilane isomers, respectively. As a consequence, the hydrogen and silyl fragments on the hydrosilylated products arise from two different silane molecules.

Experimental

Synthesis. All experiments were carried out under an atmosphere of argon using Schlenk techniques or glovebox. Solvents were obtained from a Solvent Purification System (Innovative Technologies). CD_2Cl_2, benzene-d_6, and toluene-d_8 (Euriso-top) were dried using activated molecular sieves. MeOH-d_4 (<0.02% D_2O, Euriso-top) was used as received.

[IrH(κ^3-hqca)(coe)] (**1**) was prepared from [Ir(μ-OH)(coe)$_2$]$_2$ and 8-hydroxyquinoline-2-carboxylic acid (H_2hqca) following the procedure recently described.[25] Alkynes and hydrosilanes were generally obtained from Aldrich©, except Et_3Si-C≡CH, HSiMe_2Ph (Lancaster) and *t*-Bu-Si-C≡CH (Acros Organics). All reagents were used as received without further purification.

Scientific Equipment. Elemental analyses were carried out in a Perkin-Elmer 2400 CHNS/O analyzer. NMR spectra were recorded on Bruker AV-400 and AV-300 spectrometers. Chemical shifts are reported in ppm relative to tetramethylsilane and referenced to partially deuterated solvent resonances. Coupling constants (*J*) are given in Hertz. Spectral assignments were achieved by combination of ^{1}H-^{1}H COSY, NOESY, ^{13}C DEPT and APT, ^{1}H-^{13}C HSQC and ^{1}H-^{13}C HMBC experiments. Electrospray mass spectra (ESI-MS) were recorded on a Bruker MicroTof-Q using sodium formiate as reference. MALDI-Tof mass spectra were obtained on a Bruker Miocroflex mass spectrometer using DCTB (*trans*-2-[3-(4-*tert*-butylphenyl)-2-methyl-2-propenylidene]malononitrile) or dithranol as matrix. FT-IR spectra were collected on a Nicolet Nexus 5700 FT spectrophotometer equipped with a Nicolet Smart Collector diffuse reflectance accessory. Gas chromatography/mass spectrometry (GC/MS) analysis were performed on an Agilent 7673 GC autosampler system with an Agilent 5973 MS detector operating in EI ionization method at 70 eV, equipped with an apolar capillary column Phenomenex ZB-5HT (0.25 um film thickness, 30 m x 0.25 mm i.d.).

Reaction of [IrH(κ^3-hqca)(coe)] (1) with Alkynes. General Procedure. A solution of [IrH(κ^3-hqca)(coe)] (**1**) in THF (30-40 mL) was treated with 5 equiv of the appropriate alkyne and the mixture stirred for 48 h at room temperature. The resulting dark red solution was evaporated under vacuum to give the corresponding compounds [Ir(κ^3-hqca)(alkenyl)(coe)] as red solids. In some cases a chromatographic purification step was

required. Thus, the crude compound was dissolved in CH_2Cl_2/MeOH and then transferred to an alumina column (10 × 1.5 cm). Elution with CH_2Cl_2/MeOH (10:1) gave red solutions of the complexes from which the compounds were obtained as red solids by removing the solvent under vacuum. Numbering scheme for the 8-oxidoquinoline-2-carboxylate ligand is provided in Figure 8.

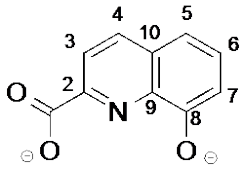

Figure 8. Numbering scheme for NMR data.

[Ir(κ^3-hqca)(*E*-CH=CHCH$_2$OMe)(coe)] (2). [IrH(κ^3-hqca)(coe)] (**1**) (0.083 g, 0.170 mmol) and 3-methoxy-1-propyne (0.68 mmol, 60 μL), chromatography purification. Yield: 67% (0.064 g). Anal. Calcd for $C_{22}H_{26}IrNO_4$: C, 47.13; H, 4.67; N, 2.50. Found: C, 47.05; H, 4.51; N 2.39. MS (MALDI, CH_2Cl_2/MeOH, m/z): 560.1 $[M]^+$, 490.0 [M – alkenyl]$^+$. ^{1}H NMR (400.162 MHz, 298 K, CD_2Cl_2/MeOH-d_4): δ 8.24 (d, H, $^3J_{H\text{-}H}$ = 8.8, H-4), 7.75 (d, 1H, $^3J_{H\text{-}H}$ = 8.8, H-3), 7.45 (t, 1H, $^3J_{H\text{-}H}$ = 8.0, H-6), 7.01 (d, 1H, $^3J_{H\text{-}H}$ = 8.0, H-5), 6.92 (d, 1H, $^3J_{H\text{-}H}$ = 8.0, H-7) (hqca), 6.83 (d, 1H, $^3J_{H\text{-}H}$ = 14.7, Ir-C*H*=CH-), 5.12 (m, 2H, =CH, coe), 4.56 (dt, 1H, $^3J_{H\text{-}H}$ = 14.6, 7.3, Ir-CH=C*H*-), 3.61 (d, 2H, $^3J_{H\text{-}H}$ = 6.6, >CH_2), 2.85 (s, 3H, -OCH_3), 2.25-2.12 (bm, 2H), 2.02-2.11 (bm, 2H), 1.85-1.95 (bm, 2H), 1.59-1.73 (bm, 2H), 1.37-1.57 (bm, 2H), (>CH_2, coe). ^{13}C{^{1}H} NMR (75.468 MHz, 298 K, CD_2Cl_2/MeOH-d_4): δ 168.61 (C-8), 141.31 (C-2), 139.42 (C-9), 134.81 (C-6), 131.41 (C-4), 129.95 (C-10) (hqca), 126.91 (Ir-CH=*C*H-), 119.15 (C-3), 113.42 (C-5), 111.36 (C-7) (hqca), 106.81 (Ir-*C*H=CH-), 86.67, 86.31 (=CH, coe), 71.53 (>CH_2), 53.54 (-O*C*H$_3$), 28.45, 28.39, 24.47 (2C), 22.82, 22.77 (>CH_2, coe). IR (ATR, cm^{-1}): ν(CO), 1650, 1614 (s).

[Ir(κ^3-hqca)(*E*-CH=CH(CH$_2$)$_3$CH$_3$)(coe)] (3). [IrH(κ^3-hqca)(coe)] (**1**) (0.196 g, 0.400 mmol) and 1-hexyne (2.0 mmol, 240 μL). Yield: 98% (0.225 g). Anal. Calcd for $C_{24}H_{30}IrNO_3$: C, 50.33; H, 5.28; N, 2.45. Found: C, 50.40; H, 5.12; N, 2.37. MS (MALDI, CH_2Cl_2/MeOH, m/z): 605.9 $[M + MeOH]^+$, 572.0 $[M]^+$, 490.1 $[M – alkenyl]^+$, 380.8 $[M – alkenyl – coe]^+$. ^{1}H NMR (300.13 MHz, 298 K, CD_2Cl_2/MeOH-d_4): δ 8.22 (d, 1H, $^3J_{H-H}$ = 8.6, H-4), 7.75 (d, 1H, $^3J_{H-H}$ = 8.7, H-3), 7.45 (t, 1H, $^3J_{H-H}$ = 8.0, H-6), 7.01 (d, 1H, $^3J_{H-H}$ = 8.1, H-5), 6.91 (d, 1H, $^3J_{H-H}$ = 7.9, H-7), (hqca), 6.17 (d, 1H, $^3J_{H-H}$ = 14.5, Ir-C*H*=CH-), 5.11 (m, 2H, =CH, coe), 4.30 (dt, 1H, $^3J_{H-H}$ = 14.5, 6.9, Ir-CH=C*H*-), 2.21 (2H), 2.05 (2H), 1.96-1.76 (6H), 1.69 (1H), 1.61-1.37 (3H), 0.98-0.76 (4H), (>CH_2), 0.57 (t, 3H, $^3J_{H-H}$ = 6.9, -CH_3). ^{13}C{^{1}H} NMR (75.468 MHz, 298 K, CD_2Cl_2/MeOH-d_4): δ 171.01 (C-8), 143.81 (C-2), 141.93 (C-9), 137.12 (C-6), 133.79 (C-4) (hqca), 133.50 (Ir-CH=*C*H-), 132.54 (C-10), 121.59 (C-3), 115.85 (C-7), 113.90 (C-5), (hqca), 100.21 (Ir-*C*H=CH-), 88.92, 88.31, (=CH, coe), 33.88 (2C), 32.82 (>CH_2), 30.98, 30.91, 26.98, 25.33, 25.23, 21.61 (>CH_2, coe), 13.50 (s, -CH_3). IR (ATR, cm^{-1}): ν(CO), 1628, 1613 (s).

[Ir(κ^3-hqca)(*E*-CH=CD(CH$_2$)$_3$CH$_3$)(coe)] (3-*d*$_1$). [IrH(κ^3-hqca)(coe)] (**1**) (0.050 g, 0.102 mmol) was dissolved in a mixture of THF (30 mL) and MeOH-d_4 (0.5 mL) and the solution stirred at room temperature for 10 minutes. 1-hexyne (0.5 mmol, 60 μL) was added and then stirred for 48 h at room temperature. Removal of solvents under vacuum afforded the compound as a red solid. Yield: 96 % (0.056 g). ^{1}H NMR (300.13 MHz, CD_2Cl_2/MeOH-d_4): δ 6.16 (s, 1H, Ir-C*H*=CD-). ^{13}C{^{1}H} NMR (75.468 MHz, CD_2Cl_2/MeOH-d_4): δ 133.46 (t, $^1J_{C-D}$ = 26.6, Ir-CH=*C*D-), 100.06 (Ir-*C*H=CD-) (selected resonances).

[Ir(κ^3-hqca)(*E*-CH=CH(CH$_2$)$_5$CH$_3$)(coe)] (4). [IrH(κ^3-hqca)(coe)] (**1**) (0.100 g, 0.204 mmol) and 1-octyne (1.0 mmol, 150 μL). Yield: 95 % (0.117 g). Anal. Calcd for $C_{26}H_{34}IrNO_3$: C, 51.98; H, 5.70; N, 2.33. Found: C, 51.80; H, 5.61; N, 2.45. MS (MALDI, CH_2Cl_2/MeOH, m/z): 600 $[M]^+$, 489.90 $[M – alkenyl]^+$. ^{1}H NMR (300.13 MHz, 298 K,

CD_2Cl_2/MeOH-d_4): δ 8.22 (d, 1H, $^3J_{H-H}$ = 8.6, H-4), 7.76 (d, 1H, $^3J_{H-H}$ = 8.5, H-3), 7.46 (t, 1H, $^3J_{H-H}$ = 7.8, H-6), 7.01 (d, 1H, $^3J_{H-H}$ = 8.1, H-5), 6.92 (d, 1H, $^3J_{H-H}$ = 8.0, H-7) (hqca), 6.19 (d, 1H, $^3J_{H-H}$ = 14.4, Ir-C*H*=CH-), 5.13 (m, 2H, =CH, coe), 4.32 (dt, 1H, $^3J_{H-H}$ = 14.4, 6.5, Ir-CH=C*H*-), 2.23 (m, 2H), 2.07 (m, 2H), 2.01-1.77 (m, 4H), 1.69 (2H), 1.61-1.37 (m, 4H), 1.11-0.75 (m, 8H) (>CH_2, coe and alkenyl), 0.71 (t, 3H, $^3J_{H-H}$ = 7.0 -CH_3). $^{13}C\{^1H\}$ NMR (75.468 MHz, 298 K, CD_2Cl_2/MeOH-d_4): δ 170.98 (C-8), 143.78 (C-2), 137.08 (C-6), 133.79 (C-4) (hqca), 133.46 (Ir-CH=*C*H-), 132.50 (C-10), 121.60 (C-3), 115.83 (C-7), 113.88 (C-5) (hqca), 100.29 (Ir-*C*H=CH-), 88.89, 88.30 (=CH, coe), 34.08 (>CH_2, coe), 31.83 (>CH_2, alkenyl), 30.97, 30.90 (>CH_2, coe), 30.44, 28.17 (>CH_2, alkenyl), 26.97 (2C), 25.31, 25.23 (>CH_2, coe), 22.87 (>CH_2, alkenyl), 13.87 (-CH_3). IR (ATR, cm^{-1}): ν(CO), 1612 (s).

[Ir(κ^3-hqca)(*E*-CH=CH(C)(CH$_3$)$_3$)(coe)] (5). [IrH(κ^3-hqca)(coe)] (**1**) (0.100 g, 0.204 mmol) and 3,3-dimethyl-1-butyne (1.0 mmol, 124 μL), chromatography purification. Yield: 62% (0.072 g). Anal. Calcd for $C_{24}H_{30}IrNO_3$: C, 50.33; H, 5.28; N, 2.45. Found: C, 50.41; H, 5.17; N, 2.33. MS (MALDI, CH_2Cl_2/MeOH, m/z): 606.2 $[M + MeOH]^+$, 574.3 $[M]^+$, 490.2 $[M – alkenyl]^+$. ^1H NMR (400.16 MHz, 298 K, CD_2Cl_2/MeOH-d_4): δ 8.21 (d, 1H, $^3J_{H-H}$ = 8.8, H-4), 7.75 (d, 1H, $^3J_{H-H}$ = 8.8, H-3), 7.45 (t, 1H, $^3J_{H-H}$ = 8.0, H-6), 7.01 (d, 1H, $^3J_{H-H}$ = 8.0, H-5), 6.92 (d, 1H, $^3J_{H-H}$ = 8.1, H-7) (hqca), 6.19 (d, 1H, $^3J_{H-H}$ = 14.7, Ir-C*H*=CH-), 5.08 (m, 2H, =CH, coe), 4.33 (d, 1H, $^3J_{H-H}$ = 14.6, Ir-CH=C*H*-), 2.19 (m, 2H), 2.05 (m, 2H), 1.89 (m, 2H), 1.68 (m, 2H), 1.58-1.40 (m, 4H), (>CH_2, coe), 0.59 (s, 9H, -CH_3). $^{13}C\{^1H\}$ NMR (75.468 MHz, 298 K, CD_2Cl_2/MeOH-d_4): δ 170.96 (C-8, hqca), 144.78 (Ir-CH=*C*H-), 143.74 (C-2), 141.90 (C-9), 137.06 (C-6), 133.75 (C-4), 132.53 (C-10), 121.54 (C-3), 115.85 (C-7), 113.87 (C-5) (hqca), 93.82 (Ir-*C*H=CH-), 88.97, 88.27 (=CH, coe), 33.24 (-*C*(CH$_3$)$_3$), 30.97, 30.92 (>CH_2, coe), 30.10 (s, 3C, -CH_3), 30.05, 27.00, 25.35, 25.25 (>CH_2, coe). IR (ATR, cm^{-1}): ν(CO), 1629, 1613.

[Ir(κ^3-hqca)(*E*-CH=CHCH$_2$OCH$_3$)(coe)(py)] (2-py). Pyridine (0.5 mL) was added to a solution of [Ir(κ^3-hqca)(*E*-CH=CHCH$_2$OMe)(coe)] (**2**) (0.112 g, 0.200 mmol) in THF (20 mL) to give an orange solution after stirring at room temperature for 14 h. The volatiles were removed under reduced pressure and the residue dissolved in the minimum amount of CH_2Cl_2 (5 mL). Addition of *n*-pentane (20 mL) led to the precipitation of an orange solid, which was washed with *n*-pentane (3×5 mL) and dried under vacuum. Yield: 97% (0.124 g). Anal. Calcd for $C_{27}H_{31}IrN_2O_4$: C, 50.69; H, 4.88; N, 4.38. Found: C, 50.52; H, 5.01; N, 4.42. MS (ESI, CH_3CN, m/z): 639.4 $[M - H]^+$, 561.4 $[M - py]^+$. ^{1}H NMR (400.162 MHz, 298 K, CD_2Cl_2): δ 8.55 (dt, 2H, $^3J_{H\text{-}H}$ = 4.8, $^4J_{H\text{-}H}$ = 1.8, *o*-H, py), 8.01 (d, 1H, $^3J_{H\text{-}H}$ = $J_{H\text{-}H}$ = 8.6, H-4, hqca), 7.68 (tt, 1H, $^3J_{H\text{-}H}$ = $J_{H\text{-}H}$ = 7.8, $^4J_{H\text{-}H}$ =1.8, *p*-H, py), 7.63 (d, 1H, $^3J_{H\text{-}H}$ = 8.8, H-3), 7.46 (t, 1H, $^3J_{H\text{-}H}$ = 7.8, H-6) (hqca), 7.28 (td, 2H, $^3J_{H\text{-}H}$ = 6.3, 4.5, *m*-H, py), 7.01 (d, 1H, $^3J_{H\text{-}H}$ = 7.8, H-5, hqca), 7.00 (d, 1H, $^3J_{H\text{-}H}$ = 14.4, Ir-C*H*=CH-), 6.90 (d, 1H, $^3J_{H\text{-}H}$ = 8.1, H-7, hqca), 5.16 (m, 2H, =CH, coe), 4.82 (dt, 1H, $^3J_{H\text{-}H}$ = 15.2, 6.6, Ir-CH=C*H*-), 3.66 (m, 2H, >CH_2, alkenyl), 2.90 (s, 3H, -CH_3), 2.13 (m, 4H), 1.90-1.77 (m, 2H), 1.75-1.44 (m , 4H), 1.39-1.26 (m, 2H) (>CH_2, coe). ^{13}C{^{1}H} NMR (75.468 MHz, 298 K, CD_2Cl_2): δ 175.04 (C=O), 171.12 (C-8) (hqca), 149.11 (2C, py), 142.78 (C-2), 141.71 (C-9) (hqca), 138.26 (py), 136.27 (C-6), 133.40 (C-4), 132.14 (C-10) (hqca), 130.02 (Ir-CH=*C*H-), 125.59 (2C, py), 121.58 (C-3, hqca), 118.65 (Ir-*C*H=CHCH-), 115.68 (C-7), 113.07 (C-5) (hqca), 87.70, 87.66 (=CH, coe), 74.94 (>CH_2), 56.17 (-OCH_3), 30.90, 30.84, 26.74, 26.72, 26.17, 26.11 (>CH_2, coe). IR (ATR, cm^{-1}): ν(CO), 1672.

[Ir(κ^3-hqca)(*E*-CH=CHCH$_2$OCH$_3$)(coe)(PPh$_3$)] (2-PPh$_3$). PPh_3 (0.110 g, 0.420 mmol) and [Ir(κ^3-hqca)(*E*-CH=CHCH$_2$OMe)(coe)] (**2**) (0.112 g, 0.200 mmol) were reacted in THF (30 mL) for 3 h. Work up as described above afforded the compound as a yellow solid. Yield: 69%: (0.114 g). Anal. Calcd for $C_{40}H_{41}IrNO_4P$: C, 50.38; H, 5.02; N, 1.70. Found: C, 50.26; H, 4.75; N, 1.65. MS (MALDI, CH_2Cl_2, m/z): 715.2 $[M - coe]^+$, 487.1 $[M - PPh_3 - alkenyl]^+$.

^{1}H NMR (400.162 MHz, 298 K, CD_2Cl_2): δ 7.72 (d, 1H, $^{3}J_{H-H}$ = 8.6, H-4, hqca), 7.30-7.10 (m, 17H, 2H of hqca and 15H of PPh_3), 6.79 (dd, 1H, $^{3}J_{H-H}$ = 15.4, $^{3}J_{H-P}$ = 6.8, Ir-C*H*=CH-), 6.76 (d, 1H, $^{3}J_{H-H}$ = 7.8, H-5), 6.66 (d, 1H, $^{3}J_{H-H}$ = 7.8, H-7) (hqca), 5.40 (m, 1H), 5.20 (m, 1H) (=CH, coe), 4.74 (ddt, $^{3}J_{H-H}$ = 15.4 and 6.5, $^{4}J_{H-P}$ = 8.0, Ir-CH=C*H*-), 3.50 (dd, 2H, $^{3}J_{H-H}$ = 6.5, $^{5}J_{H-P}$ = 2.0, >CH_2, alkenyl), 2.64 (s, 3H, -CH_3), 2.12 (br m, 2H), 1.98 (br m, 1H), 1.90 (br m, 1H), 1.77 (br m, 2H), 1.13-1.05 (br m, 6H) (>CH_2, coe). ^{13}C{^{1}H} NMR (75.468 MHz, 298 K, THF-d_8): δ 174.09 (C=O), 172.45 (C-8), 143.53 (C-2), 143.37 (C-9) (hqca), 138.13 (d, $^{2}J_{C-P}$ = 113.6, Ir-*C*H=CHCH-), 136.64 (C-6, hqca), 135.34, (d, 2C, $^{2}J_{C-P}$ = 10, PPh_3), 133.77 (C-4, hqca), 133.44 (C-10, hqca), 131.49 ($^{4}J_{C-P}$ = 2.2, PPh_3), 130.61 (d, $^{1}J_{C-P}$ = 35.6, PPh_3), 129.57 (d, 2C, $^{3}J_{C-P}$ = 9, PPh_3), 127.81 (Ir-CH=*C*H-), 122.78 (C-3), 115.86 (C-5), 113.32 (C-7) (hqca), 85.85, 84.80, (=CH, coe), 76.12 (d, J_{C-P} = 12.7, >CH_2), 56.39 (-CH_3) (alkenyl), 32.25, 31.96, 27.85, 27.74, 27.21, 26.27 (>CH_2, coe). ^{31}P{^{1}H} NMR (161.99 MHz, 298 K, CD_2Cl_2): δ -11.25 (s). IR (ATR, cm^{-1}): ν(CO), 1676 (s).

[Ir(κ^3-hqca)(*E*-CH=CHCH$_2$OMe)(coe)(CO)] (2-CO). Carbon monoxide was bubbled through a solution of [Ir(κ^3-hqca)(*E*-CH=CHCH$_2$OMe)(coe)] (**2**) (0.040 g) in MeOH-d_4/CD_2Cl_2 (1 mL) at room temperature for 1h and the resulting solution transferred to NMR tube. ^{1}H NMR (300.13 MHz, 298 K, CD_2Cl_2): Selected resonances for **2-CO**, δ 8.35 (d, 1H, $^{3}J_{H-H}$ = 8.7, H-4), 7.84 (d, 1H, $^{3}J_{H-H}$ = 8.7, H-3), 7.59 (t, 1H, $^{3}J_{H-H}$ = 8.2, H-6), 7.15 (d, 1H, $^{3}J_{H-H}$ = 8.2, H-5), 7.08 (d, 1H, $^{3}J_{H-H}$ = 8.2, H-7) (hqca), 6.45 (d, 1H, $^{3}J_{H-H}$ = 15.4, Ir-C*H*=CH-), 5.35 (m, 3H, =CH coe and Ir-CH=C*H*-). IR (CH_2Cl_2, cm^{-1}): ν(CO), 2035 (s).

General Procedure for Hydrosilylation of 1-alkynes. A NMR tube was charged under argon with the catalyst precursor (1.54 x 10^{-3} mmol, 2 mol %), $CDCl_3$ (0.5 mL), the corresponding alkyne (0.077 mmol) and silane (0.085 mmol). The solution was kept in a thermostatic bath at 60 °C and monitored by ^{1}H NMR spectroscopy. The vinylsilane reaction products were unambiguously characterized on the basis of the coupling patterns and

constants of vinylic protons in the ^{1}H NMR spectra and subsequent comparison to literature values.[31] Values for *J* ranged from 17-19 Hz for β-(*E*), 13-16 Hz for β-(*Z*) and 1-3 Hz for α vinylsilanes.

Calculation details. DFT calculations have been carried out with Gaussian 09[32] using the B3LYP functional. For Ir atoms the lanl2dz and its associated basis set supplemented[33] with an f function was used and the 6-31G** basis set from the rest of atoms. Methylacetylene was used as a model of the alkyne substrates and trimethylsilane a silane model. Energies are reported in the discussion in terms of enthalpy. All the stationary structures have been characterized by frequency calculations. For transition structures a single imaginary frequency was found and additional IRC calculations in both directions of the transition vector were performed to ensure the connection to the related endpoints. When the IRC calculations finished before reaching the minima, additional optimization were performed from the endpoint reached so far.

Author Information

Corresponding Authors. E-mails: perez@unizar.es, modrego@unizar.es

Note. The authors declare no competing financial interests.

Acknowledgments. Financial support from the Ministerio de Economía y Competitividad (MINECO/FEDER) of Spain (Project CTQ2013-42532-P) and Diputación General de Aragón (DGA/FSE E07) is gratefully acknowledged. R. P-O. acknowledges her fellowship from MINECO (BES-2011-045364). The authors gratefully acknowledge the resources from the supercomputer "Caesaraugusta" (node of the Spanish Supercomputer Network) and the technical expertise and assistance provided by BIFI-Universidad de Zaragoza.

Supporting Information. Electronic energy, enthalpy, free energy in gas phase and optimized coordinates for catalytic intermediates and transition states; multinuclear NMR

data and GC/MS of the hydrosilylation of 1-ethynyl-4-(trifluoromethyl)benzene with triethylsilane, and reaction profile of the isomerization of β-(*Z*)-PhCH=CHSiMe$_2$Ph catalyzed by **1**. This material is available free of charge via the Internet at http://pubs.acs.org.

References

(1) (a) Marciniec, B. In *Applied Homogeneous Catalysis with Organometallic Compounds*; Cornils, B., Herrmann, W. A., Eds.; Wiley-VCH: Weinheim, Germany, 2002; Vol. 1. (b) Marciniec, B. In *Hydrosilylation: A Comprehensive Review on Recent Advances*; Matisons, J., Ed.; Springer: New York, 2009; pp 53−123.

(2) (a) Ojima, I. In *The Chemistry of Organic Silicon Compounds*; Patai, S.; Rappoport, Z., Eds.; Wiley: New York, 1989; pp 1479−1526. (b) Ojima, I.; Li, Z.; Zhu, J. In *The Chemistry of Organic Silicon Compounds*; Rappoport, Z., Apeloig, Y., Eds.; Wiley: NewYork, 1998; Vol. 2, pp 1687−1792.

(3) (a) Meister, T. K.; Riener, K.; Gigler, P.; Stohrer, J.; Herrmann, W. A.; Kühn, F. E. *ACS Catal*. **2016**, *6*, 1274–1284. (b) Harrod, J. F.; Chalk, A. J. *J. Am. Chem. Soc*. **1965**, *87*, 1133−1133. (c) Chalk, A. J.; Harrod, J. F. *J. Am. Chem. Soc*. **1965**, *87*, 16−21.

(4) (a) Hamze, A.; Provot, O.; Brion, J.-D.; Alami, M. *J. Organom. Chem*. **2008**, *693*, 2789–2797. (b) Silbestri, G. F.; Flores, J. C.; de Jesús, E. *Organometallics* **2012**, *31*, 3355−3360. (c) Berthon-Gelloz, G.; Schumers, J.-M.; De Bo, G.; Markó, I. E. *J. Org. Chem*. **2008**, *73*, 4190−4197. (d) De Bo, G.; Berthon-Gelloz, G.; Tinant, B.; Markó, I. E. *Organometallics* **2006**, *25*, 1881–1890. (e) Aneetha, H.; Wu, W.; Verkade, J. G. *Organometallics* **2005**, *24*, 2590–2596. (f) Doyle, M. P.; High, K. G.; Nesloney, C. L.; Clayton, J. W.; Lin, J. *Organometallics* **1991**, *10*, 1225–1226. (g) Lewis, L. N.; Sy, K. G.; Bryant, G. L.; Donahue, P. E. *Organometallics* **1991**, *10*, 3750–3759.

(5) (a) Iglesias, M.; Aliaga-Lavrijsen, M.; Sanz Miguel, P. J.; Fernández-Alvarez, F. J.; Pérez-Torrente, J. J.; Oro, L. A. *Adv. Synth. Catal*. **2015**, *357*, 350–354. (b) Busetto, L.; Cassani, M. C.; Femoni, C.; Mancinelli, M.; Mazzanti, A.; Mazzoni, R.; Solinas; G. *Organometallics* **2011**, *30*, 5258–5272. (c) Jiménez, M. V.; Pérez-Torrente, J. J.; Bartolomé, M. I.; Gierz, V.; Lahoz, F. J.; Oro, L. A. *Organometallics* **2008**, *27*, 224–234. (d) Zeng, J. Y.; Hsieh, M. H.; Lee, H. M. *J. Organomet. Chem.* **2005**, *690*, 5662–5671. (e) Sato, A.; Kinoshita, H.; Oshima, K. *Org. Lett.* **2004**, *6*, 2217-2220. (f) Poyatos, M.; Mas-Marzá, E.; Mata, J. A.; Sanaú, M.; Peris, E. *Eur. J. Inorg. Chem.* **2003**, 1215–1221. (g) Faller, J. W.; D'Alliessi, D. G. *Organometallics* **2002**, *21*, 1743–1746. (h) Doyle, M. P.; High, K. G.; Nesloney, C. L.; Clayton, T. W., Jr.; Lin, J. *Organometallics* **1991**, *10*, 1225-1226. (i) Takeuchi, R.; Nitta, S.; Watanabe, D. *J. Chem. Soc., Chem. Commun.* **1994**, 1777-1778. (j) Milan, A.; Fernandez, M. -J.; Bentz, P.; Maitlis, P. M. *J. Mol. Catal*. **1984**, *26*, 89–104 (k) Hill, J. E.; Nile, T. A. *J. Organomet. Chem.* **1977**, *137*, 293-300. (l) Watanabe, H.; Kitahara, T.; Motegi, R.; Nagai, Y. *J. Organomet. Chem.* **1977**, *139*, 215-222.

(6) (a) Iglesias, M.; Pérez-Nicolás, M.; Sanz Miguel, P. J.; Polo, V.; Fernández-Alvarez, F. J.; Pérez-Torrente, J. J.; Oro, L. A. *Chem. Commun*. **2012**, *48*, 9480–9482. (b) Zanardi, A.; Peris E.; Mata, J. A. *New J. Chem*. **2008**, *32*, 120–126. (c) Miyake, Y.; Isomura, E.; Iyoda, M. *Chem. Lett.* **2006**, *35*, 836–837. (d) Shimizu, R.; Takamasa F. *Tetrahedron Lett*. **2000**, *41*, 907–910.

(7) (a)Viciano, M.; Mas-Marza, E.; Sanau, M.; Peris, E. *Organometallics* **2006**, *25*, 3063–3069. (b) Mas-Marza, E.; Sanau, M.; Peris, E. *Inorg. Chem.* **2005**, *44*, 9961–9967. (c) Mas-Marza, E.; Poyatos, M.; Sanau, M.; Peris, E. *Inorg. Chem.* **2004**, *43*, 2213–2219.

(8) (a) Dragutan, V.; Dragutan, I.; Delaude, L.; Demonceau, A. *Coord. Chem. Re*v. **2007**, *251*, 765–794. (b) Menozzi, C.; Dalko, P. I.; Cossy, J. *J. Org. Chem.* **2005**, *70*, 10717–10719. (c) Maifeld, S. V.; Tran, M. N.; Lee, D. *Tetrahedron Lett.* **2005**, *46*, 105–108. (d) Nagao, M.; Asano, K.; Umeda, K.; Katayama, H.; Ozawa, F. *J. Org. Chem.* **2005**, *70*, 10511–10514. (e) Arico, C. S.; Cox, L. R. *Org. Biomol. Chem.* **2004**, *2*, 2558-2562. (f) Katayama, H.; Taniguchi, K.; Kobayashi, M.; Sagawa, T.; Minami, T.; Ozawa, F. *J. Organomet. Chem.* **2002**, *645*, 192. (g) Martín, M.; Sola, E.; Lahoz, F. J.; Oro, L. A. *Organometallics* **2002**, *21*, 4027–4029. (h) Na, Y.; Chang, S. *Org Lett.* **2000**, *2*, 1887-1889.

(9) Tanke, R. S.; Crabtree, R. H. *J. Am. Chem. Soc.* **1990**, *112*, 7984–7989.

(10) Ojima, I.; Clos, N.; Donovan, R. J.; Ingallina, P. *Organometallics* **1990**, *9*, 3127–3133.

(11) (a) Chung, L. W.; Wu, Y.-D.; Trost, B. M.; Ball, Z. T. *J. Am. Chem. Soc*. **2003**, *125*, 11578–11582. (b) Trost, B. M.; Ball, Z. T. *J. Am. Chem. Soc*. **2003**, *125*, 30–31. (c) Trost, B. M.; Ball, Z. T. *J. Am. Chem. Soc*. **2001**, *123*, 12726–12727.

(12) Iglesias, M.; Sanz Miguel, P.; Polo, V.; Fernández-Alvarez, F. J.; Pérez-Torrente, J. J.; Oro, L. A. *Chem. Eur. J.* **2013**, *19*, 17559−17566.

(13) (a) Bergens, S. H.; Noheda, P.; Whelan, J.; Bosnich, B. *J. Am. Chem. Soc.* **1992**, *114*, 2128–2135. (b) Lachaize, S.; Sabo-Etienne, S.; Donnadieu, B.; Chaudret, B. *Chem. Commun.* **2003**, 214–215. (c) Cervantes, J.; Gonzalez-AlaTorre, G.; Rohack, D.; Pannell, K. H. *Appl. Organomet. Chem.* **2000**, *14*, 146–151. (d) Itami, K.; Mitsudo, K.; Nishino, A.; Yoshida, J. *J. Org*. Chem. **2002**, *67*, 2645–2652. (e) Maruyama, Y.; Yamamura, K.; Sagawa, T.; Katayama, H.; Ozawa, F. *Organometallics* **2000**, *19*, 1308–1318. (f) Maruyama, Y.; Yamamura, K.; Nakayama, I.; Yoshiuchi, K.; Ozawa, F. *J. Am. Chem. Soc.* **1998**, *120*, 1421–1429.

(14) Vicent, C.; Viciano, M.; Mas-Marzá, E.; Sanaú, M.; Peris, E. *Organometallics* **2006**, *25*, 3713–3720.

(15) (a) Gao, R.; Pahls, D. R.; Cundari, T. R.; Yi, C. S. *Organometallics* **2014**, *33*, 6937–6944. (b) Yan, Y.-F.; Chung, L. W.; Zhang, X.; Houk, K. N.; Wu, Y.-D. *J. Org. Chem*. **2014**, *79*, 8856–8864. (c) Ding, S.; Song, L. J.; Chung, L. W.; Zhang, X.; Sun, J. *J. Am. Chem. Soc.* **2013**, *135*, 13835–13842.

(16) (a) Wang, W.; Gu, P.; Wang, Y.; Wei, H. *Organometallics* **2014**, *33*, 847-857. (b) Wu, Y.; Karttunen, V. A.; Parker, S.; Genest, A.; Rösch, N. *Organometallics* **2013**, *32*, 2363–2372. (c) Tuttle, T.; Wang, D.; Thiel, W.; Kohler, J.; Hofmann, M.; Weis, J. *Dalton Trans.* **2009**, *30*, 5894–5901. (d) Sakaki, S.; Sumimoto, M.; Fukuhara, M.; Sugimoto, M.; Fujimoto, H.; Matsuzaki, S. *Organometallics* **2002**, *21*, 3788–3802.

(17) (a) Gao, P.; Guo, W.; Xue, J.; Zhao, Y.; Yuan, Y.; Xia, Y.; Shi, Z. *J. Am. Chem. Soc.* **2015**, *137*, 12231–12240. (b) Huang, G. P.; Kalek, M.; Liao, R. Z.; Himo, F. *Chem. Sci.* **2015**, *6*, 1735–1746. (c) Appelhans, L. N.; Zuccaccia, D.; Kovacevic, A.; Chianese, A. R.; Miecznikowski, J. R.; Macchioni, A.; Clot, E.; Eisenstein, O.; Crabtree, R. H. *J. Am. Chem. Soc*. **2005**, *127*, 16299–16311. (d) Oxgaard, J.; Muller, R. P.; Goddard, W. A., III; Periana, R. A. *J. Am. Chem. Soc*. **2004**, *126*, 352–363. (e) Webster, C. E.; Hall, M. B. *Coord. Chem. Rev*. **2003**, *238–239*, 315–331. (f) Tamura, H.; Yamazaki, H.; Sato, H.; Sakaki, S. *J. Am. Chem. Soc*. **2003**, *125*, 16114–16126. (g) Klei, S. R.; Tilley, T. D.; Bergman, R. G. *J. Am. Chem. Soc*. **2000**, *122*, 1816–1817.

(18) (a) Cheng, C.; Kim, B. G.; Guironnet, D.; Brookhart, M.; Guan, C.; Wang, D. Y.; Krogh-Jespersen, K.; Goldman, A. S. *J. Am. Chem. Soc*. **2014**, *136*, 6672–6683. (b) Mazuela, J.; Norrby, P.-O.; Andersson, P. G.; Pàmies, O.; Diéguez, M. *J. Am. Chem. Soc*. **2011**, *133*,

13634–13645. (c) Hopmann, K. H.; Bayer, A. *Organometallics* **2011**, *30*, 2483–2497. (d) Church, T. L.; Rasmussen, T.; Andersson, P. G. *Organometallics* **2010**, *29*, 6769–6781. (e) Cui, X.; Fan,Y.; Hall, M. B.; Burgess, K. *Chem. -Eur. J.* **2005**, *11*, 6859–6868. (f) Brandt, P.; Hedberg, C.; Andersson, P. G. *Chem. -Eur. J.* **2003**, *9*, 339–347.

(19) (a) Metsänen, T. T.; Hrobárik, P.; Klare, H. F. T.; Kaupp, M.; Oestreich, M. *J. Am. Chem. Soc.* **2014**, *136*, 6912–6915. (b) Park, S.; Brookhart, M. *Organometallics* **2010**, *29*, 6057–6064.

(20) Sridevi, V. S.; Fan W. Y.; Leong, W. K. *Organometallics* **2007**, *26*, 1157–1160.

(21) (a) *Pincer and Pincer-Type Complexes: Applications in Organic Synthesis and Catalysis*; Szabo, K. J.; Wendt, O. F., Eds.; Wiley-VCH: Weinheim, 2014. (b) *The Chemistry of Pincer Compounds*; Morales-Morales, D., Jensen, C. M., Eds.; Elsevier: Amsterdam, 2007.

(22) (a) O'Reilly, M. E.; Veige, A. S. *Chem. Soc. Rev.* **2014**, *43*, 6325−6369. (b) Szigethy, G.; Heyduk, A. F. *Dalton Trans.* **2012**, *41*, 8144− 8152. (c) Heyduk, A. F.; Zarkesh, R. A.; Nguyen, A. I. *Inorg. Chem.* **2011**, *50*, 9849−9863. (d) Fu, R.; Bercaw, J. E.; Labinger, J. A. *Organometallics* **2011**, *30*, 6751−6765. (e) Zarkesh, R. A.; Heyduk, A. F. Organometallics **2011**, *30*, 4890−4898. (f) Weinberg, D. R.; Hazari, N.; Labinger, J. A.; Bercaw, J. E. *Organometallics* **2010**, *29*, 89−100.

(23) (a) Bhalla, G.; Lui, X. Y.; Oxgaard, J.; Goddard, W. A.; Periana, R. A. J. *Am. Chem. Soc.* **2005**, *127*, 11372−11389. (b) Tanke, R. S.; Crabtree, R. H. *Organometallics* **1991**, *10*, 415−418. (c) Tanke, R. S.; Crabtree, R. H. *J. Chem. Soc., Chem. Commun*. **1990**, 1056−1057.

(24) (a) Nguyen, D. H.; Greger, I.; Pérez-Torrente, J. J.; Jiménez, M. V.; Modrego, F. J.; Lahoz, F. J.; Oro, L. A. *Organometallics* **2013**, *32*, 6903−6917. (b) Nguyen, D.H.; Pérez-

Torrente, J .J.; Lomba, L.; Jiménez, M. V.; Lahoz, F. J.; Oro, L. A. *Dalton Trans*. **2011**, *40*, 8429−8435.

(25) Nguyen, D. H.; Pérez-Torrente, J. J.; Jiménez, M. V.; Modrego, F. J.; Gómez-Bautista, D.; Lahoz, F. J.; Oro, L. A. *Organometallics* **2013**, *32*, 6918–6930.

(26) (a) Paredes, P.; Díez, J.; Gamasa, M. P. *J. Organom. Chem*. **2008**, *693*, 3681–3687. (b) She, L.; Li, X.; Sun, H.; Ding, J.; Frey, M.; Klein, H.-F. *Organometallics* **2007**, *26*, 566−570. (c) Li, X.; Vogel, T.; Incarvito, C. D.; Crabtree, R. H. *Organometallics* **2005**, *24*, 62–76. (d) Marchenko, A. V.; Gérard; H. Eisenstein, O.; Caulton. K. G. *New J. Chem*. **2001**, *25*, 1244–1255. (e) Bassetti, M.; Casellato, P.; Gamasa, M. P.; Gimeno, J.; González-Bernardo, C.; Martín-Vaca, B. *Organometallics* **1997**, *16,* 5470–5477.

(27) Mori, A.; Takahisa, E.; Yamamura, Y.; Kato, T.; Mudalige, A. P.; Kajiro, H.; Hirabayashi, K.; Nishihara, Y.; Hiyama, T. *Organometallics* **2004**, *23*, 1755–1765.

(28) Paris, S. I. M.; Lemke, F. R. *Inorg. Chem. Commun*. **2005**, *8*, 425–428.

(29) (a) Poater, A.; Pump, E.; Vummaleti, S. V. C.; Cavallo, L. *J. Chem. Theor. Comput.* **2014**, *10*, 4442-4448. (b) Li, B.; Bi, S.; Liu, Y.; Ling, B.; Li, P. *Organometallics* **2014**, *33*, 3453-3463. (c) Hatanaka, M.; Morokuma, K. *J. Am. Chem. Soc.* **2013**, *135*, 13972-13979. (d) Liang, Y.; Liu, S.; Xia, Y.; Li, Y.; Yu, Z.-X. *Chem. - Eur. J.* **2008**, *14*, 4361-4373. (e) Sakaki, S.; Takayama, T.; Sumimoto, M.; Sugimoto, M. *J. Am. Chem. Soc.* **2004**, *126*, 3332-3348. (f) Strajbl, M.; Sham, Y. Y.; Villà, J.; Chu, Z.-T.; Warshel, A. *J. Phys. Chem. B* **2000**, *104*, 4578-4584. (g) Martin, R. L.; Hay, P. J.; Pratt, L. R. *J. Phys. Chem.: A* **1998**, *102*, 3565-3573. (h) Mammen, M.; Shakhnovich, E. I.; Deutch, J. M.; Whitesides, G. M. *J. Org. Chem.* **1998**, *63*, 3821-3830.

(30) (a) Crabtree, R. H. *New J. Chem.* **2003**, *27*, 771-772. (b) Frohnapfel, D. S.; Templeton, J. L. *Coord. Chem. Rev.* **2000**, *206*, 199-235. (c) Casey, C. P.; Brady, J. T.; Boller, T. M.; Weinhold, F.; Hayashi, R. K. *J. Am. Chem. Soc.* **1998**, *120*, 12500-12511.

(31) See for example: (a) Derivates from *n*-Bu-C≡CH. Jun, C. H.; Crabtree, R. H. *J. Organomet. Chem.* **1993**, *447*, 177–187. (b) Derivates from *n*-Hex-C≡CH. Nakamura, S.; Uchiyama, M.; Ohwada, T. *J. Am. Chem. Soc.* **2004**, *126*, 11146–11147. (c) Derivates from *t*-Bu-C≡CH. Andavan, G. T. S.; Bauer, E. B.; Letko, C. S.; Hollis, T. K.; Tham, F. S. *J. Organomet. Chem.* **2005**, *690*, 5938–5947. (d) Derivates from Et_3SiC≡CH. Sudo, T.; Asao, N.; Gevorgyan, V.; Yamamoto, Y *J. Org. Chem.* **1999**, *64*, 2494–2499. (e) Derivates from Ph-C≡CH. Katayama, H.; Taniguchi, K.; Kobayashi, M.; Sagawa, T.; Minami, T.; Ozawa, F. *J. Organomet. Chem.* **2002**, *645*, 192–200. (f) Derivates from 4-MeO-C_6H_4-C≡CH. Hamze, A.; Provot, O.; Brion, J.-D.; Alami, M. *J. Organomet. Chem.* **2008**, *693*, 2789–2797. (g) Derivates from 4-CF_3-C_6H_4-C≡CH. Hamze, A.; Provot, O.; Brion, J.-D.; Alami, M. *Synthesis* **2007**, 2025–2036.

(32) Frisch, M. J.; Trucks, G. W.; Schlegel, H. B.; Scuseria, G. E.; Robb, M. A.; Cheeseman, J. R.; Scalmani, G.; Barone, V.; Mennucci, B.; Petersson, G. A.; Nakatsuji, H.; Caricato, M.; Li, X.; Hratchian, H. P.; Izmaylov, A. F.; Bloino, J.; Zheng, G.; Sonnenberg, J. L.; Hada, M.; Ehara, M.; Toyota, K.; Fukuda, R.; Hasegawa, J.; Ishida, M.; Nakajima, T.; Honda, Y.; Kitao, O.; Nakai, H.; Vreven, T.; Montgomery Jr, J. A.; Peralta, J. E.; Ogliaro, F.; Bearpark, M. J.; Heyd, J.; Brothers, E. N.; Kudin, K. N.; Staroverov, V. N.; Kobayashi, R.; Normand, J.; Raghavachari, K.; Rendell, A. P.; Burant, J. C.; Iyengar, S. S.; Tomasi, J.; Cossi, M.; Rega, N.; Millam, N. J.; Klene, M.; Knox, J. E.; Cross, J. B.; Bakken, V.; Adamo, C.; Jaramillo, J.; Gomperts, R.; Stratmann, R. E.; Yazyev, O.; Austin, A. J.; Cammi, R.; Pomelli, C.; Ochterski, J. W.; Martin, R. L.; Morokuma, K.; Zakrzewski, V. G.; Voth, G. A.;

Salvador, P.; Dannenberg, J. J.; Dapprich, S.; Daniels, A. D.; Farkas, Ö.; Foresman, J. B.; Ortiz, J. V.; Cioslowski, J.; Fox, D. J. Gaussian, Inc., Wallingford CT (USA), **2013**.

(33) Ehlers, A. W.; Bohme, M.; Dapprich, S.; Gobbi, A.; Hollwarth, A.; Jonas, V.; Kohler, K. F.; Stegmann, R.; Veldkamp, A.; Frenking, G. *Chem. Phys. Lett.* **1993**, *208*, 111-114.